

In uence of non-m agnetic im purities on hole doped two-leg Cu-O Hubbard ladders

P. Chudzinski^{1,2}, M. Gabay² and T. Giamarchi¹

¹ DPMCM-ANEP, University of Geneva, 24 Quai Ernest-Ansermet CH-1211 Geneva, Switzerland

² Laboratoire de Physique des Solides, Bat. 510, Université Paris-Sud 11, Centre d'Orsay, 91405 Orsay Cedex, France

Abstract.

We study the influence of non magnetic impurities on the phase diagram of doped two-leg Hubbard Cu-O ladders. In the absence of impurities this system possesses d-wave superconducting states and orbital current states depending on the doping. A single, strong, scatterer modifies its environment locally and this effect is assessed using a renormalization group analysis. At high doping, disorder causes intraband instabilities and at low doping it promotes interband instabilities. In the former case, we extend the boundary conformal field theory method (developed in the context of single chains) to handle the ladder problem, and we find exact closed-form analytical expressions for the correlation functions. This allows us to compute experimentally measurable local quantities such as the nuclear magnetic resonance line broadenings and scanning tunnelling microscope profiles. We also discuss the low doping regime where Kondo physics is at play, making qualitative predictions about its nature. Insight into collective effects is also given in the many weak impurities case, based on an RG approach. In this regime, one sees the interplay between interactions and disorder. We emphasize the influence of the O atoms on disorder effects both for the single- and for the many-defect situations.

1. Introduction

Despite intensive efforts, the interplay between interactions and superconductivity in low dimensional systems is still poorly understood. An especially important question, considering the case of high T_c compounds, is whether interactions are responsible for the unusually high superconducting temperatures in these materials. In addition to this issue, there is a considerable debate on the appropriate choice of a minimal model needed to describe these compounds. A remarkable situation when these questions can be studied in a controlled fashion is the one dimensional limit of ladder materials [1]. Indeed, in one dimension, powerful theoretical tools [2] allow a detailed analysis of interactions effects [3, 4, 5, 6, 7, 8, 9, 10]. It was shown, for a single band model, that ladders exhibit a form of d-wave superconductivity driven by purely repulsive interactions, and this result is suggestive that a similar physics might be at play in their higher dimensional counterpart. In addition to their interest in connection with the cuprates, ladders have spawned their own field, thanks to the existence of several experimental realizations [11, 12, 13, 14, 15].

In addition to the superconducting phase, many questions touch upon the normal phase in these superconducting systems and in particular the topic of the so called pseudogap phase. Various explanations have been put forward, ranging from preformed superconducting pairs [16] to the existence of orbital currents with [17] or without [18, 19] broken translational symmetry. Recent neutrons experiments [20, 21] indicating the presence of magnetic moments, compatible with translationally invariant pattern of currents, and Kerr effect measurements [22] showing evidence of time-reversal symmetry breaking have generated a large interest in this topic. Although current (ux) phases have been first proposed for the single-band Hubbard model [23, 16, 24, 25], they have been found unstable in slave bosons and numerical calculations. Ladders have also provided a controlled environment to study this important issue. It was found that somewhat special interactions, more complex than local ones, are needed to stabilize them [26, 27]. The resulting phases break the translational symmetry of the lattice, leading to a staggered ux pattern. Similar staggered patterns were advocated as a potential explanation of the pseudogap phase [17] (DDW phase).

In order to find new phases it thus seemed necessary to go beyond the single band model [18, 19]. For ladders, this was done both at half filling [28] when the system is insulator and more recently [29, 30] using a renormalization procedure, for arbitrary doping. Quite remarkably for finite doping, a new massless phase, absent in the case of a single band Hubbard ladder and able to sustain orbital currents was found. A detailed investigation of the properties of this new phase, and more generally of a three band model for a ladder system is thus a challenging and interesting question.

One way to access the properties of such a phase is to probe its response to the presence of impurities. Indeed, when defects are present, translational symmetry is broken and momentum is not a good quantum number anymore. Wavefunctions with different momenta mix and, at low temperature, the static ($\omega = 0$) response contains contributions from large momentum states. Investigations of correlation effects using impurities was largely done for insulating ladders. Nuclear magnetic resonance (NMR) experiments performed by Takigawa et. al. [31] showed that non-magnetic impurities broaden the NMR lines, which then display a distinctive temperature dependence. This finding confirmed earlier theoretical predictions [32]. Subsequently, various families of low dimensional models with different characteristics (dimerization, zig-zag)

were investigated theoretically [33]. In the vicinity of an impurity, and in the ground state, two distinct generic behaviors were found 1) a magnetic state is exponentially localized near the defect 2) a delocalized antiferromagnetic (AF) cloud surrounds the defect (for temperatures on the order of 100K, the polarization extends over tens of lattice spacings). The former case corresponds to systems in which magnetic degrees of freedom are gapped (e.g. the Haldane spin 1 chain [34]) while the latter case corresponds to an ungapped situation (e.g. the spin 1=2 chain or the pseudo-gap state of two-dimensional systems). Both behaviors were found experimentally. For instance, on the basis of an NMR study on ladders, the authors of Ref. [35] claimed that the temperature dependence of the line broadening could be explained by the former (gapped) case for very small concentrations of defects and by the latter (ungapped) case for larger concentrations. Similar results and conclusions were reported in the work of Ref. [36], on the basis of NMR and NQR measurements. From the amplitude of the broadened part, both sets of authors concluded that the AF cloud has to extend over surprisingly many unit cells.

On the theoretical side, Laukamp et al. [33] performed numerical studies of 1D spin models, including spin ladders. They observed that, quite generally, the magnetic response of the system contains a large staggered part near an isolated defect. Further computational work was done by Lauchli et al. [37], who studied the nature of the states around a Li atom impurity substituting a copper site in a single orbital Cu ladder. They found a triplet bound state but suggested that free spinons could be obtained when several defects are present or with other types of impurities. The former case is suggestive of the overscreened free spin scenario which is usually discussed in the context of the density matrix renormalization group (DMRG) analysis of two-leg spin ladders [33]. The latter case signals that, even with a vanishingly small density of defects, spinons will gain kinetic energy and delocalize rather than form a local bound state inside the energy gap, close to the impurity. These two different regimes were also observed in studies of the quasiclassical sine-Gordon model [38]. The bound spin state limit was investigated analytically, using a Majorana fermion technique [39]. The authors of that study stated the conditions under which this regime might exist and computed the additional contribution to the susceptibilities stemming from the bound state. The properties of soliton states at the boundary (i.e. next to the defect) { including magnetic susceptibilities { were discussed in detail in a series of papers by Essler [40, 41].

In this work, we consider the problem of impurities in doped two-leg Cu-O Hubbard ladders for which both the superconducting phases and the novel orbital current phases are present. In the defect-free case, the phase diagram as a function of carrier doping was established in Refs. [29, 30]. Such a system is characterized by two energy bands controlling the fluctuations of (two) charge and (two) spin modes near the Fermi energy. Three different regimes were found: 1) strong gaps in the spin modes and in one of the charge modes at low doping; 2) a Luttinger liquid (LL) (gapless) phase at intermediate doping; 3) gapless charge modes, no gap for one of the spin mode and a small gap for the other at higher doping. Because the most significant perturbation caused by impurities is the mixing of the two bands we can expect this effect to be the largest in the last two doping ranges where interactions promote band separation in the absence of disorder. By contrast, in the ground state of the clean system at low doping, the two bands strongly mix so that the perturbation is expected to be less "dangerous" and the physics of the lightly doped ladder should be qualitatively similar to that of the disordered (undoped) spin ladder. For this

reason, we will be mostly concerned in this paper with the regime of intermediate and large carrier content. For large dopings, in the absence of disorder, the size of the gap in the spin sector is small, so that, for experimentally relevant temperatures, it does not play a role, and the state is effectively described by a LL. Hence, from this point on, we focus on the role of disorder in the LL phase of moderately and highly doped Cu-O ladders. We will consider two extreme situations, for impurities, namely the case of a single impurity producing a strong scattering potential on the one hand and the case of a finite concentration of defects producing each a weak scattering potential, on the other.

Our paper is organized as follows: in Sect. 2, we present the model which describes the physics of a doped two-leg Cu-O Hubbard ladder. In the continuum limit the quadratic part of the Hamiltonian is diagonal in a particular basis where it takes the simple form of a sum of LL modes. The relevant notation used in the course of this paper is introduced at that stage. We recall the characteristics of the phase diagram in the absence of disorder. The Hamiltonian modelling the scattering by a single, strong impurity is then expressed in terms of bosonic phase fields.

In Sec. 3, we generalize the boundary conformal field theory (BCFT) methods { which have been successfully used in the context of chains { to handle the two-leg ladder problem. The possible fixed points of the RG flows are given in the presence of disorder, and their stability is discussed. Then, the generalized boundary conditions for the phase fields are derived, at the open boundary condition (OBC) fixed point.

Sec. 4 presents our main results for the single impurity case. Only local properties of the system are affected, and, when we are considering LL phases at intermediate and high dopings, the bulk parameters K_i (the compressibilities) remain unchanged. We generalize the procedure developed by Eggert and Aleck [32, 42] to treat the two-band case. Green functions and alternating magnetizations in the vicinity of the impurity are computed. χ_{alt} , the alternating part of the (local) susceptibility is predicted to cause NMR Knight shift broadenings K , and the changes in the imaginary part of the Green function ought to be detectable in scanning tunnelling microscopy (STM) measurements of the local spectral weights (LSW). We study their temperature dependence in order to provide experimentally testable predictions. Possible differences stemming from the location of the impurity within the unit cell or outside of the ladder are discussed.

In Sec. 5, for the sake of completeness, we consider various limiting situations. First we discuss the nature of the states in the low doping phase. Next, we examine the rigidity of intermediate, gapless phase, and consider a putative instability of the bulk phase in the vicinity of the impurity. The competition between disorder and interactions is discussed in terms of RG arguments. Finally, in the presence of many impurities acting collectively, we analyse the RG flow leading to Anderson localization.

We conclude, with an experimental perspective on the use of non-magnetic impurities as a probe of correlated ground states in such ladder systems.

2. The model

We consider a two-leg Cu-O ladder with an impurity. The Hamiltonian of this system contains three parts: the kinetic energy of electrons moving on the lattice H_T , electron interactions H_{int} and an impurity term H_{imp}

$$H = H_T + H_{int} + H_{imp} \quad (1)$$

The physics of the first two terms is known [29, 30]. In the first part of this section, we briefly recall its main characteristics, and we also introduce relevant notations. In the second part, we express the impurity Hamiltonian using the standard bosonization description of one dimensional systems [2].

2.1. The clean ladder

Including two Cu and one O atoms in the unit cell, the tight-binding kinetic energy part H_T reads

$$H_T = \sum_j \sum_{m \in 2Cu} \left(\sum_{m \in 2O} t_{co} n_{mj} + \sum_{m \in 2Cu} t_{cc} \sum_{\sigma} a_{mj}^\sigma (b_{m,j} + b_{m,j-1}) + h.c. \right) + \sum_{m \in 2O} \left(\sum_{m \in 2Cu} t_{oc} \sum_{\sigma} b_{mj}^\sigma (a_{m+1,j} + a_{m-1,j}) + h.c. \right) + \sum_{m \in 2Cu} \left(\sum_{m \in 2O} t_{pp} \sum_{\sigma} b_{mj}^\sigma (b_{m+1,j} + b_{m-1,j} + b_{m+1,j-1} + b_{m-1,j-1}) + h.c. \right) \quad (2)$$

where a_{mj} (b_{mj}) is the creation operator of holes with spin σ on a copper (oxygen) site (j is a site along chain and m labels the atoms in each cell); $n_{mj}^{Cu} = a_{mj}^{Cu\dagger} a_{mj}^{Cu}$. We use hole notation such that t, t_c, t_{pp} are all positive. $t_{co} = \epsilon_o - \epsilon_{Cu}$ is the difference between the oxygen and copper on-site energies.

Eigenvalues and eigenvectors of the non-interacting part are simply obtained through a Fourier transform of H_T . If ϵ is of the same order as or larger than the hopping t , one may neglect the non-bonding and antibonding high energy states which have mostly a p-type character, and this reduces the model to two low lying bands crossing the Fermi energy. They are denoted ϕ (symmetric under the exchange of the two legs) and ψ (antisymmetric under the exchange of the two legs). With $\epsilon = 0$ and σ denoting the band and the spin index respectively, the Hamiltonian reads

$$H_T = \sum_k \epsilon(k) n_k \quad (3)$$

where

$$a_{mk} = \sum_m a_{mk} \quad (4)$$

and $\epsilon(k)$ and a_{mk} are the eigenvalues and components of the eigenvectors of the Hamiltonian matrix (see Ref. [30]).

In the low energy limit one may linearize the dispersion relation in the vicinity of the Fermi energy:

$$H_T = \sum_{\sigma} \sum_{q \in Q} v_F a_{\sigma q}^\dagger a_{\sigma q} \quad (5)$$

and it is easy to bosonize this free fermion theory [2, 43]. Two (charge and spin) boson phase fields denoted by $\phi(x)$ are introduced for each fermion species. ϕ denotes both spin and band indexes, x is the spatial coordinate along the ladder. Fermionic operators are written as $\psi = \exp(i(\phi + \theta))$ where θ are the Klein factors which satisfy the required anticommutation relations for fermions. These θ do not contain any spatial dependence and they commute with the Hamiltonian operator. They only influence the form of the order operators in bosonic language (through contributions

ϕ_j) and the signs of the non-linear couplings via coefficients (eigenvalues of ϕ_j operators). $\phi_j^2 = 1$ and in this paper we choose the convention $\phi_j = +1$, as in Ref. [44].

We also introduce the phase field θ_j ; its spatial derivative $\partial_x \theta_j$ is canonically conjugated with ϕ_j . Now the Hamiltonian may be rewritten using the above phase fields. The kinetic part and those pieces in H_{int} which can be expressed as density-density terms give rise to the following form

$$H_0 = \sum_{\mathbf{r}} \sum_{\sigma} \frac{dx}{2} [(u - K_{\sigma}) (\partial_x \theta_j)^2 + \left(\frac{u}{K}\right) (\partial_x \phi_j)^2] \quad (6)$$

For the non-interacting system one has $K_{\sigma} = 1$ for all modes; the diagonal density basis is then the bonding/antibonding one B_0 (the momentum k_z associated with the rungs is either 0 or π). The other basis which is commonly used in the literature is the total/transverse one, B_+ . It is related to B_0 in such a way that:

$$\phi_j(\sigma) = \frac{\phi_j^0}{2} \quad (7)$$

where σ represents a spin or a charge index, depending on which particular density one considers.

The interaction part, in fermionic language, is given by

$$H_{int} = \sum_{j,m} \sum_{\sigma} (U_{Cu} n_{m,j\sigma} n_{m,j\sigma} + U_O n_{m,j\sigma} n_{m,j\sigma} + \sum_{m \neq 0} \sum_{\sigma} V_{Cu-O} n_{m,j\sigma} n_{n,j\sigma}) \quad (8)$$

The bosonized form of Eq. (8) contains terms of the density-density type. As we mentioned above, these are included in the \hat{K} matrix, and hence they are treated exactly in this procedure. Since the form of \hat{K} depends on the basis in which the densities are expressed, the Hamiltonian will take the simple form Eq. (6) in the eigenbasis of the matrix \hat{K} . The remaining interaction terms yield non-linear cosines and these are the ones for which the RG procedure is required. In Refs. [29, 30] we showed that the eigenbases for the spin and for the charge modes rotate during the RG flow. Two fixed points were found, namely B_+ and B_0 . Interband physics dominates in the former case (mixing of the σ and π bands) and intraband physics, in the latter case. Close to half filling (low doping regime), B_+ is the fixed point basis for the spin and the charge modes. Both spin modes are gapped, and so is one of the charge modes. Using the notation of Balents and Fisher [9] the ladder is in the C1S0 state (CnSm denotes n (m) gapless charge (C) (spin S) modes). For an intermediate range of dopings, B_+ is the fixed point basis for the spin variables and B_0 the fixed point basis for the charge variables. This is the C2S2 regime when all modes are gapless. The decoupling of the spin and of the charge eigenbasis is responsible for this quantum critical state. For higher dopings, B_0 is the fixed point basis for the spin and the charge modes. The ladder is in the C2S1 phase where the σ spin mode is gapped. The corresponding phase diagram is shown in Fig.1.

2.2. Bosonization of a single impurity

Let us consider a two-leg Cu-O ladder with a single defect located in the unit cell positioned at $x = 0$. It could be a vacancy, an interstitial, or even a distortion caused

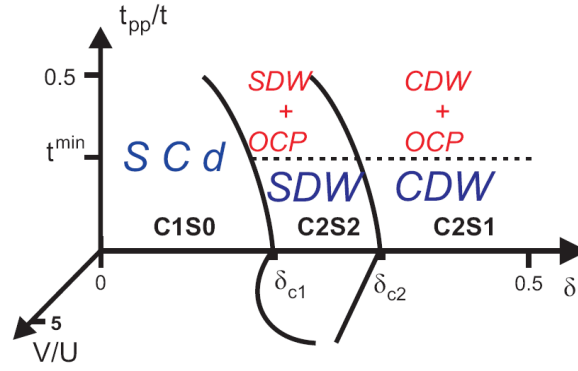


Figure 1. The phase diagram of two-leg Cu-O Hubbard ladders versus doping for $U_{Cu} > 0$. Zero doping corresponds to the half-filled case. The umklapp terms which open a gap in the charge symmetric mode are not included here

by the electrostatic potential of some external source (i.e. not located on the ladder). A sketch of such impurity is shown in figure 3 and its generic scattering effect is depicted in figure 2. Such a defect obviously affects the motion of carriers along the ladder. In 1D, there are simply two possibilities for scattering on an impurity: forward and backward. In fermionic language this leads to a contribution of the form

$$H_{imp} = \sum_{q=0}^X V_{for}(x=0) \sum_k^Y \frac{1}{k+q} \psi_k(0) + \sum_{q=2k_F}^X V_{bac}(x=0) \sum_k^Y \frac{1}{k+q} \psi_k(0) \quad (9)$$

The two terms, in the rhs of Eq. (9) are totally decoupled and thus can be treated independently. The strategy is to rewrite them in a bosonic phase field language, using the appropriate substitution

2.2.1. Forward scattering In the bosonic representation, we find that forward scattering acts like an additional chemical potential: $V(0) \psi^\dagger(x=x_0)$. It is well known that this effect can be accounted for by shifting the phase fields in the spin sector by an amount proportional to the value of the potential: $\phi_i \rightarrow \phi_i + \frac{K}{V_1} V(0)$, where $V(0)$ is the strength of the forward scattering on an impurity sitting at $x=0$. We conclude that, for a single impurity problem, the expectation value of the field at $x=0$ remains unchanged; it does not influence the analysis of the backscattering part. In principle, forward scattering effects may thus be omitted. However, a proviso is in order.

As we are dealing with two bands, we get three independent shifts (two from intraband and one from interband forward scattering); these can be factored out, with the help of the appropriate basis rotation. Anticipating the analysis of backscattering terms, where a similar rotation of the basis will be introduced, the following statement can be made: as long as forward and backward interband scattering are equal (which is a reasonable assumption) there won't be any inconsistency in our procedure. This consideration is important, for example, for the calculation of correlation functions at finite temperature, where the OBC fixed point is not reached yet. In the discussion of backscattering, we may distinguish two limiting behaviors: reflection from a non-magnetic boundary or coupling to a spin state localized around the impurity. We devote most of our attention to the former case, since it corresponds to the LL regime

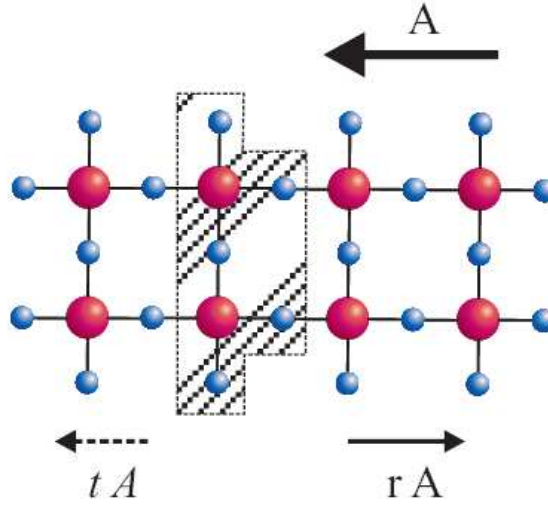


Figure 2. A schematic rendition of the scattering event caused by a single impurity: a left moving wave, denoted by A , impinges upon the shadowed region, where an impurity is located. A portion, rA , is backscattered (the process described by a reflection matrix), and the rest, tA , is transmitted to the other side. For moderate or high dopings, the latter process only takes place at non-zero temperature.

that we are focusing on in this work. For the spin (bound) state case, Kondo-like forward scattering terms must be taken into account.

2.2.2. Backward scattering The second part, in the rhs of Eq. (9), is more involved, because, in the bosonic representation, it produces non-linear terms. In the case of a two-leg ladder, the situation is even more complicated than for the single chain, since there are now two different types of backscattering processes – a reflection within a given band and a reflection from one band to the other.

The intraband contribution reads

$$H_o^{(imp)} = V_o \cos(\phi_{so}) \cos(\phi_{co}) \Big|_{k=0} = V_o \cos\left(\frac{\phi_s + \phi_{s+}}{2}\right) \cos\left(\frac{\phi_c + \phi_{c+}}{2}\right) \Big|_{k=0} \quad (10)$$

and

$$H^{(imp)} = V \cos(\phi_s) \cos(\phi_c) \Big|_{k=0} = V \cos\left(\frac{\phi_s}{2}\right) \cos\left(\frac{\phi_c}{2}\right) \Big|_{k=0} \quad (11)$$

The interband contribution, expressed in the B_+ basis (appropriate to treat band-mixing processes) is

$$H_o^{imp} = V_o \cos(\phi_{s+}) \cos(\phi_{c+}) \cos(\phi_s) \cos(\phi_c) \Big|_{k=0} \quad (12)$$

The influence of these non-linear terms will be discussed in the next section, using an RG analysis. Their relevance signals that backward scattering is strong enough to "cut" the ladder. We will show that this entails important changes in the expression of correlation functions.

3. Field theory for the impurity problem

In this section we describe the low energy properties of the ladder in the presence of an impurity. Two steps are required: first, one should determine, using RG, the fixed points of the problem and solve an open boundary problem; second, from the fermionic boundary conditions (reflection and mixing amplitudes) one should determine the proper boundary conditions for the bosonic phase fields. This is precisely the order in which the present section is organized. Within each of its subsections we consider in sequence the C1S0, C2S2 and C2S1 phases, which were obtained in the case of a defect-free ladder.

3.1. RG flows and fixed points

The RG calculation for the single impurity problem proceeds in two steps: first one takes the unperturbed ladder and adds the impurity backscattering potential to check its possible relevance. When the impurity potential is relevant, one makes an educated guess about the fixed point of the RG flow. The second step consists in checking the stability of this strong coupling fixed point.

3.1.1. Weak coupling The RG differential equations for the backscattering potential can be derived using the standard procedure of integrating out high energy degrees of freedom. One should simply bear in mind [45, 46] that, since, V is a local process at $x = 0$, the scaling variable is simply the time coordinate. The RG flow can be monitored so long as V can be treated as a perturbation. Two important technical remarks are in order, before we write down the RG equations and discuss their solutions. They play an important role in the subsequent analysis.

One concerns the initial conditions that one chooses at the start of the flow. In the unit cell of the Cu-O ladders, there are several atoms, and hence various possible configurations, when an impurity is included. One could consider the substitution of one of the Cu atoms (the a_1 d-orbital in figure 3) by Zn (a non magnetic ion) which creates a highly asymmetric defect, as shown in figure 3(a). Alternatively, an oxygen atom could move away from its equilibrium position, causing a distortion, or even could be removed from the structure. In that respect, the on-rung, central (p-orbital indicated as b_0) oxygen atom stands out: this type of site is encountered in ladders and in two-dimensional (2D) cuprate materials. Such a term preserves the reflection symmetry with respect to the two legs that one has in the case of a non disordered ladder. This is shown in Fig. 3(b). The outer and on-leg oxygen sites (b_2 and b_1 orbitals respectively) are a bit more difficult to analyze, because in real systems, where there is usually some residual coupling between neighboring ladders, they introduce some mixing between ladders. Distortions that extend over a few unit cells or removing of apical oxygen can be thought of as symmetric obstacles. The reflection amplitudes for the different types of impurities will be evaluated in Sec. 4.

Symmetry (or lack of thereof) with respect to the exchange of the two legs of the ladder is a critical issue. The corresponding symmetry axis is noted σ . The asymmetric case induces a strong initial band mixing process. By contrast, a defect that sits exactly at the position of an on-rung oxygen atom does not produce an initial band-mixing. This shows that the presence of oxygen atoms in the unit cell impacts the symmetry breaking properties of the impurity. Of course, one is required to check whether or not this property is preserved during the flow. If it is not, i.e. if band mixing,

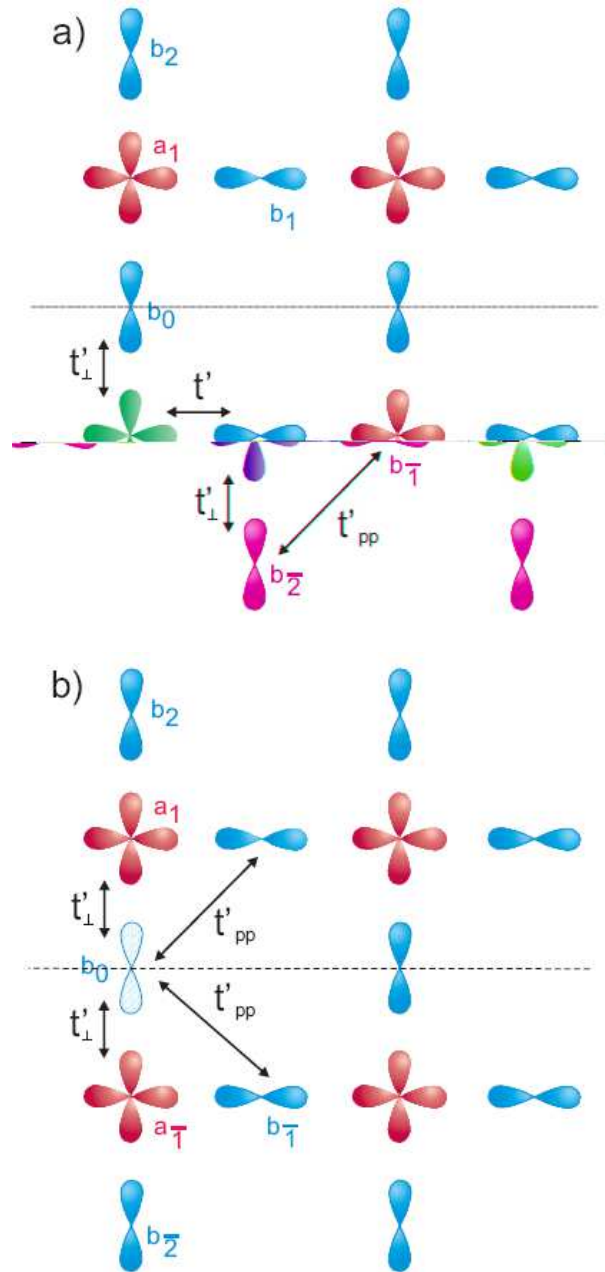


Figure 3. An atomic view of the unit cell where a defect (in green) is located. In an elementary cell, an impurity can be either "asymmetric" (a) or "symmetric" (b). A "symmetric" defect preserves the symmetry with respect to the axis along the ladder, shown as a dashed line and denoted \hat{y} in the text. The hopping amplitudes which are affected by the presence of the impurity are shown in each case

backward scattering, terms become relevant during the flow, one may conclude that symmetry breaking has occurred. Thus the fixed point ground state phase should be strongly asymmetric. More generally, the RG procedure may enhance or lower the local symmetry of the system (by suppressing or reinforcing the influence of interband backscattering). Such direct link between RG and symmetries is often postulated, but it is not always as clearly seen as in the present case. For the Cu-O ladder, it shows already in real space: because of symmetry breaking, the dominant instability which arises close to impurity should promote a difference between the two legs.

We introduce here such type of instability, as it will recur frequently in the course of our paper. An obvious example, in the particle-hole channel, is the so called π -density wave (π -DW) which takes the following forms in language of fermions (operator $\psi = \psi_{\sigma} \chi_{\sigma}$ with chirality, band and spin indexes) and bosonic fields:

$$\begin{aligned} O_{CDW} = & \frac{1}{2} \sum_{\sigma} \sum_{\sigma'} \sum_{\sigma''} \sum_{\sigma'''} \psi_{\sigma}^{\dagger} \psi_{\sigma'} \psi_{\sigma''} \psi_{\sigma'''} \cos \frac{q_c}{2} \cos \frac{q_s}{2} \cos \frac{q_{c+s}}{2} \cos \frac{q_{c-s}}{2} \sin \frac{q_c}{2} \cos \frac{q_c}{2} \sin \frac{q_s}{2} \sin \frac{q_{c+s}}{2} \sin \frac{q_{c-s}}{2} \end{aligned} \quad (13)$$

where $q_c = \pi$, $q_s = 0$ (or π) if $\sigma = \uparrow$ (or \downarrow), and the \cos and \sin symbols in the l.h.s of Eq. (13) refer to left and right moving fermions, respectively. In real space it corresponds to a characteristic pattern, which will be called "zig-zag pattern" in the course of the paper.

The second remark concerns the impact of the impurity potential on the RG flow of the LL parameters. Since a single impurity may not change the thermodynamic properties of the system we can use the fact that the flows of $K_i(l)$ and $g_i(l)$ are not affected by the presence of the impurity far enough from it, and one can simply use results known for the defect-free bulk. Since we are working in a regime when the initial values of the backscattering terms are much stronger than that of interactions (but such that they can still be treated as perturbations), the RG step should be done as follows, in order to obtain the proper flow for $V_i(l)$: one should take the functions $K_i(l)$ and $g_i(l)$ that were obtained in the absence of disorder and plug them into the differential equations obeyed by the $V_i(l)$. Inserting instead the fixed point values K_i and g_i would work in the opposite limit of strong interactions. This procedure is meaningful provided we stay at energy scales above the gaps. At the start of the RG process, the initial strength of the backscattering potential is assumed to be small, but one has to remember that the smaller it is, the longer it takes to renormalize it to strong values (where one enters the tunnelling regime). In the following RG analysis, we assume that the initial strength of the impurity is strong enough to drive the system quickly towards the fixed point, whenever the impurity potential is a relevant perturbation. This ensures that if the impurity is relevant, then the effect induced by it will be visible (below some reasonable temperature/energy scale). Since the V_i renormalize faster than the $K_i(l)$ and the $g_i(l)$, it also ensures that there exists an energy window where the strong coupling (tunnelling) analysis of the impurity is applicable. This requirement is not fulfilled when defects are located on outer oxygen sites, or when small distortions of the bond lengths occur, so these situations have to be excluded from our analysis.

With the above mentioned considerations in mind, we now proceed to implement the RG procedure. We take into account the rotation of the eigenbases, and, depending on their fixed point, we write different sets of equations. We perform the analysis starting from the strongly doped ladder limit, and work our way towards the half-filled case.

In uence of non-magnetic impurities on hole doped two-leg Cu-O Hubbard ladders 12

C2S1 phase: at high doping, in the C2S1 phase, the intraband basis (B_0) is relevant and the differential equations describing the flow are

$$\begin{aligned}\frac{dV_0}{dl} &= V_0 (2 - K_{so}(l) - K_{co}(l)) \\ \frac{dV}{dl} &= V (2 - K_s(l) - K_c(l)) \\ \frac{dV_0}{dl} &= V_0 \left(2 - \frac{1}{4} (K_{so}^{-1}(l) + K_s^{-1}(l) + K_{so}(l) + K_s(l) \right. \\ &\quad \left. + K_{co}^{-1}(l) + K_c^{-1}(l) + K_{co}(l) + K_c(l)) \right)\end{aligned}\quad (14)$$

One sees that the V_0 backscattering term is exactly marginal to second order in perturbation. For the intraband backscattering: $d_0 = (K_{so}(l) + K_{co}(l)) < 2$, so V_0 is relevant; $d = (1 + K_c(l)) > 2$. More specially, it is less than 2 only at the beginning of the flow so V is weakly relevant or marginally relevant.

In the large doping case, the interpretation of the results of the RG analysis is quite straightforward. The relevant operators scale to infinity which signals that the intraband backscattering terms V_0 and V cut the ladder when the temperature goes to zero. One may generalize arguments used for spin chains and assume that the system flows towards the open boundary fixed point. The only difficulty is how to treat the V_0 backscattering. Although it is marginal (i.e. not relevant) one cannot simply neglect its influence, especially we cannot say that it will scale to zero at the fixed point of the flow. This bears upon the important issue of whether there is a single, stable, fixed point or a line of fixed points (controlled by V_0), which cannot be excluded by the weak coupling RG analysis. Nevertheless, contrarily to the case of the low doping limit, a solution can be found in the C2S1 regime.

C2S2 phase: at intermediate dopings, the analysis of the gapless C2S2 phase is also challenging. First of all, the charge sector is described by the intraband basis (B_0) while the spin sector, as for lower dopings, is described by the total transverse one (B_+). Besides, because of spin rotational invariance all the LL parameters K_s are equal to one. This simplifies the RG equations to

$$\begin{aligned}\frac{dV_0}{dl} &= V_0 (1 - K_{co}(l)) \\ \frac{dV}{dl} &= V (1 - K_c(l)) \\ \frac{dV_0}{dl} &= V_0 \left(1 - \frac{1}{2} (K_{co}^{-1}(l) + K_c^{-1}(l) + K_{co}(l) + K_c(l)) \right)\end{aligned}\quad (15)$$

For these equations the V_0 backscattering term is exactly marginal to second order in perturbation. For the intraband backscattering terms: $d_0 = K_{co}(l) < 1$, so V_0 is relevant and $d = K_c(l) < 1$ so V is weakly relevant.

However one should be careful when interpreting this result. The fact that the spin sector, which is crucial both at low doping (spin screening) and at high doping (spin gap), does not appear to influence the relevance of backscattering is quite puzzling. It is known [47, 48, 49] that for a critical SU(2) invariant phase, the band mixing term V_0 may cause important (in fact dominant) logarithmic corrections. These corrections favor an instability (spin screening) of the same nature as that which pertains to the C1S0 phase. In this respect the physics is similar to that discussed before for the low doping regime. Analytical studies of this problem were devoted to the case of spin

ladders, when charge modes are frozen out. Here charge modes are present and the fact that their fluctuations are described in the B_0 basis could potentially suppress the influence of the V_0 backscattering term. Thus the discussion of this intermediate phase will be postponed until the end of this paper, because we are not in a position to make exact predictions about the strong coupling fixed point in this regime, at that stage.

C1S0 phase: For the C1S0 phase (low doping case), the total/transverse basis is relevant and the differential equations describing the flow are given by

$$\begin{aligned}\frac{dV_{0=}}{dl} &= V_{0=} \left(2 - \frac{1}{2} (K_{s-}(l) + K_{s+}(l) + K_c(l) + K_{c+}(l)) \right) \\ \frac{dV_0}{dl} &= V_0 \left(2 - \frac{1}{2} (K_{s-}^{-1}(l) + K_{s+}(l) + K_c^{-1}(l) + K_{c+}(l)) \right)\end{aligned}\quad (16)$$

The V_0 backscattering term (band mixing caused by an impurity) is the simplest to analyze. K_{c+} is always much smaller than one, K_{s+} may decrease but not increase and K_c increases but may not decrease, so this backscattering operator, if it is present, is the most relevant one. The analysis pertaining to the intraband backscattering terms V_0 and V_- is a little bit more involved, as $d_0 = d = \frac{1}{2} (K_1 + K_2 + K_3 + K_4)$ is initially smaller than 2 but that, in the course of the flow, it exceeds this value. This suggests a non-monotonous evolution of the potential during the RG procedure: first it increases and then it decreases (so the overall amplitude of its variation will depend on the scale which characterizes the approach of V_0 towards unity).

Thus, the band mixing process, which takes us away from the simple four LL mode generalization of the spinful chain problem, dominates the low energy physics. In addition, intraband RG gives a non-monotonic behavior, so the initial conditions play a critical role in this case. The only statement that can be safely made is that the system flows away from the unperturbed situation. In other words, perfect transmission is an unstable fixed point of the flow in the low doping regime. We need to assess the regime towards which V_- flows. Within the range of validity of our treatment, we cannot produce a rigorous solution, but we provide below some reasonable indications.

Some statements can also be made as regards the fixed point symmetry properties. If we assume that the initial conditions of the flow are symmetric, then because V_0 is strongly relevant, any deviation from this ideal position would cause band-mixing processes. One can see that an exactly symmetric defect is also an unstable fixed point in the phase space of intra- and inter-band scatterings. The system flows towards a strongly asymmetric situation, where fluctuations affect each leg differently.

These findings have an impact on a symmetry analysis of the impurity problem: for high dopings we do not predict any enhancement of band-mixing at the fixed point; then a zig-zag pattern will be much more visible for Cu atom substitutions than for other, more symmetric, types of distortion. For all cases, intraband physics dominates, and one may apply the BCFT procedure.

To summarize, the RG analysis is not able to give a full answer to the backscattering relevance question, but we are still able to distinguish two regimes: at low dopings, interband scattering dominates, whereas, at high dopings, intraband reflection prevails. In order to apply BCFT (for the bosonic fields) one needs to have stronger intraband backscattering than band-mixing, at the fixed point. Thus, strictly speaking, our method is well suited to the high doping regime. Before setting to apply BCFT one should check the stability of the suggested fixed points.

3.1.2. Strong coupling Performing an analysis in the strong coupling regime requires some knowledge of the characteristics of the low temperature fixed point. For single chains this is an easy task, since a 1D system is either cut or not, but as we show below, this is not as straightforward for ladders. What is more, the nature the fixed point around which the analysis is performed changes from phase to phase. Thus, analyzing the effect of the impurity for each phase will be even more involved than in the weak coupling (perturbative) limit. At the end of the section we provide some arguments supporting the possible existence of "exotic" fixed points (multi-particle tunnelling processes).

C2S1 phase: Let us discuss first the large doping limit, because in this case the strong impurity fixed point is much easier to identify. On the basis of the above arguments, one may conclude that, for the C2S1 phase, there is no intermediate fixed point and the impurity simply scales to the tunnelling limit. We have then established the limits of validity of our approach, based on CFT. We will come back to this point in the discussion part (Sec. 5). We now turn to the physics at the fixed point. In the case when intraband backscattering dominates, one can use the duality procedure [45] and analyze the flow starting from the strong coupling fixed point of a weak tunnelling between two semi-infinite ladders. For single chains, it was shown, that the tunnelling problem could be solved using a saddle point approximation. The sequential tunnelling events are described in terms of a dilute instanton gas. In this duality mapping, the quadratic part which was previously the free part, is responsible for interactions between instantons. One obtains the same partition function, through the simple mapping [45] $\phi \rightarrow \phi + \frac{1}{2} \ln \phi$. It was later shown [46] that this can be generalized to the case of two diagonal (spin and charge) LL modes. In our case, when all K_i are close to one, the weak/strong impurity regimes are exactly dual and the boundaries (in K_i phase space) of these two limits coincide. We will come back to this point at the end of this section. In a similar manner one may straightforwardly generalize the analysis to the case of four LL modes. One point has, however, to be taken into consideration: for the 1D chain, spin and charge are independent degrees of freedom and, to first order, they do not mix on the boundary. By contrast, from the geometry of the ladder, one sees that the impurity usually causes some mixing of the ϕ and ψ bands: if the impurity is symmetric with respect to the ϕ axis, we cannot get any mixing, but in the generic case, when only one of the chains is cut, the chain, not the band, basis is appropriate to describe the propagation of carriers. The chain basis implies band mixing.

In the case of a symmetric barrier, the band description is still valid and we may define instantons using a saddle point approximation within each band. It is the intraband instability which corresponds to this kind of impurity, and the dominant tunnelling process is described by a term which can be treated to second order in perturbation (the first order contribution vanishes)

$$\sum_Z \int dt_1 \int dt_2 h \frac{1}{10} (\mathbf{x} = 0; t_1) \frac{1}{20} (\mathbf{x} = 0; t_1) \frac{1}{20} (\mathbf{x} = 0; t_2) \frac{1}{10} (\mathbf{x} = 0; t_2) i \quad (17)$$

This leads to the limiting situation of two independent, semi-infinite, ladders 1 and 2. The result of Ref. [46] can easily be generalized in this case, and we find an OBC stable fixed point. Of course, even at high dopings, one cannot a priori rule out the possibility of band mixing backscattering, but we may predict that the size of the effect in the tunnelling regime is similar to that calculated initially at the beginning of RG procedure.

The case when only one of the legs is cut is a little more involved. Using the same argument as before, we find that a type of instability which minimizes the energy (in the sense that it produces a zero expectation value at the position of the impurity) is now the $-$ charge density wave ($-$ CDW). It is the only type of density wave (DW) ordering which mixes the σ and π bands and it is defined within each chain, as expected. Then, the dominant type of tunnelling is expected to be of the following form: $\psi_0(x=0)\psi_2(x=0) \propto \exp(-\int_0^x \text{CDW}(t_1;t_2))$. One can now make the same exact calculation (to second order in perturbation) for this kind of process, or use the dilute instanton approximation for the $-$ CDW instantons to find an equation similar to that for V_0 , but with the $K_i \rightarrow K_i^{-1}$ mapping. Note that here are two approaches to the tunnelling problem: one treating it as a second order perturbation (see Eq. (17)) with known OBC density of states, another using quasi-classical instanton solutions. Both give the same answer. One sees then that, for high dopings, this kind of tunnelling is marginal { it will not destabilize the OBC fixed point } but it has to be taken into account in the analysis. It might seem surprising that, even if the perturbation only affects one of the legs, we end up at the reflecting fixed point anyway, but an analogy with the Fano resonance may be useful here [50, 51]. In the Fano problem, we have two channels: one with weak and one with strong transmission. If the coupling between the two is strong (as is the case here), the so-called asymmetry parameter q is equal to zero [50] and one observes a dip at the Fermi energy, which is increasingly pronounced as the temperature is reduced. Due to quantum interferences between the channels, the conductance tends to zero with decreasing energy scale (temperature, gate voltage).

Within the RG framework, we have shown so far that, for the impurity problem, there exists a stable line, toward which the flow takes us, corresponding to an intra- or an inter-band reflection. It might be desirable to address the issue of the nature of the flow on this line (for instance, if we have a line of fixed points), but this lies beyond the scope of the present work. A remark is in order here. There is always an intrinsic infrared cut-off, due to some characteristic size (inverse of the impurity concentration) or to a finite temperature; also, depending on where the impurity sits inside the unit cell, one could get marginally relevant scattering processes which strongly affect the flow. Taking these effects into account, it is safest to consider more general boundary conditions, including reflection processes of both types. Hence, we do not assume that, upon reaching the true zero temperature fixed point, one of these two types of backscattering disappears.

C2S2 phase At this point, we are not yet in a position to discuss the influence of the impurity for this phase. First, we need to investigate the low doping regime more closely. But an important statement is in order; until now we had considered that, for each doping, the phase in contact with the impurity was that of the defect-free ladder at that particular value of the doping; this might not be the case for a critical, gapless, phase which is usually very sensitive to any perturbation. We will come back to this important issue in Sec. 5 (in particular when we discuss the gapless phase).

C1S0 phase: Performing exactly the same RG analysis of all possible tunnelling terms as that described above { in the low doping phase } shows that no suppression of intraband instanton events occurs, down to the lowest temperature. In the charge sector, for temperatures $T < T_c$, we find $K_c \rightarrow 1$ (while all other $K_i \rightarrow 1$), so that

the intraband transmission coefficients $t_{\alpha\beta}$ become relevant, and this makes the OBC fixed point unstable. Only the interband t_0 is strongly suppressed which means that a DW resonance is produced around the impurity. In this case, it is desirable to identify the nature of the new, intermediate, fixed point. Note that the above statement holds only so long as the c mode remains gapped (the condition $K_c = 1$ is directly connected with this), so it should not be valid in the massless C2S2 phase.

The relevance of band-mixing terms for the low doping phase suggests that the physics is dominated by on-chain boundary states. The C1S0 phase has an SCd character, with singlet on-rung Cooper pairs. Removing one of sites leaves an unpaired free spin on the other chain. In addition, at half filling, rewriting the gapped spin sector in terms of Majorana fermions allows one to identify the boundary state as a triplet (the condition for the triplet excitation mass, $m_t > 0$, must be fulfilled [39]). Finally, from the dispersion relation of a single Cu-O chain (in a nearest neighbor tight binding model approximation), one concludes that the on-chain resonance can only exist in a low doping energy range. Extending this arguments, which holds at half-filling (strong interactions regime), to the entire C1S0 phase, suggests that for weak doping the fixed point is different from that describing a simple reflection on the boundary. Instead a bound state (exponentially decaying into the bulk) with a spin $1/2$ forms around the defect and the system flows to a different fixed point. This behavior is not quantitatively captured, in the framework of our approach (for other examples of such situation, see Ref. [49]), so we will only make some qualitative predictions.

To that end, it is worthwhile performing an RG analysis of the various Kondo-type couplings with the boundary spin-state. The general scattering operator on the impurity spin S has the following form :

$$H_{\text{b-imp}} = \sum_0^X J_K^0 (\psi \sim 0) S$$

where i is the band index (we can have either intra- or inter-band scattering in our system). The band part $(\psi \sim 0)$ can be rewritten in bosonic language, giving rise to terms proportional to $J_K^0 \exp(i \phi_{R S \pm}(x=0)) S_i$. Here, $i = z; +; -$, depending on whether the z component or spin- \uparrow processes of the impurity spin are concerned. Following Aeck, the impurity spin only couples to one chiral (right going in our case) spin field, since backscattering on the boundary is relevant.

Some details regarding the treatment of the above Kondo terms are presented in Appendix A. The most important difference between inter- and intra-band terms is the presence of a $\cos(\phi_{R C}(x=0))$ term in the former case. An RG analysis of all possible J_K^0 can be performed assuming OBC (relevance of V_0). Because of the presence of a charge transverse term ($K_c > 1$), J_K^0 is strongly relevant while the other couplings are marginally relevant. As the temperature is lowered further, we approach the energy scale for which $K_s < 1$ (which corresponds to the opening of a spin gap). In this regime all the J_K^0 couplings become irrelevant. Hence, we may write an effective Hamiltonian for the spin degrees of freedom below the charge gap ϵ_c , but above the spin gap energies ϵ_s . It describes interband Kondo scattering:

$$H_{\text{b-imp}} = J_K^0 \cos(\phi_{R S}(x=0)) S^z + J_K^0 (S^+ \exp(i \phi_{R S+}(x=0)) + \text{h.c.}) \quad (18)$$

Let us point out that, in contradiction with the usual case, it is the total spin field $\phi_{R S+}$ which is responsible for the impurity spin- \uparrow processes. The form of this spin- \uparrow term suggests that (as for a single-channel Kondo problem) bulk carriers are able

to screen the impurity spin at zero temperature. In addition, the term coupled to S^z is not of the density-density type, which is why it has a non-linear cosine form rather than the customary gradient form. Hamiltonian (18) can be mapped onto a resonant level model, albeit with an extra interaction term stemming from the z component of the spin. The above RG arguments suggest the existence of an additional, stable, intermediate fixed point in the low doping regime. It is easy to show that the J_K couplings are relevant only if B_+ is the fixed point eigenbasis, which is consistent with the existence of (impurity) spin states only at low dopings. We will explore the nature of this new state in more detail, in Sec. 5.

Exotic tunnelling processes To complete our analysis of the strong coupling limit, we need to check if additional tunnelling processes could be generated in higher order. For the case of the spin chain, Ref. [46] included the possibility of double spinon or double holon tunnelling events. Such processes dominate if the relevant LL parameter satisfy $K_i < 1=2$. In our model, there are four modes and so, obviously, many more processes of this type. Using a path integral Monte Carlo technique, the boundaries between such tunnelling regimes, for all dopings, were investigated [52] and the crossover regime between the weak and the strong impurity cases were determined. No additional intermediate fixed points was found. We would then conclude that in our model, as long as all $K_i \geq 1$, this kind of exotic tunnelling process cannot make the fixed point unstable. One might of course worry that $K_i \geq 1$ is a property that is connected with the weak coupling treatment of interactions. Fortunately, at high dopings, we can waive this concern. In that limit, the K parameters in the band have an intrinsic tendency to renormalize towards one, which means that no spinon-holon separation can be expected around the impurity. Regarding the o band the situation is more complicated: one finds that K_{so} renormalizes towards the Luther-Emery point ($K_{so} = 1=2$), and, at the same time, that interactions open up a gap in this mode (which corresponds to the freezing of spinons). On the other hand interactions push K_{∞} strongly below one; it is then quite difficult to reach a regime where double holon tunnelling will make the fixed point unstable. From the above mentioned numerical analysis [52] it appears that the region of the phase diagram where these exotic tunnelling events dominate is even more suppressed, and, for a given value of $K_{so} = 1=2$, the condition $K_{\infty} > 2$ would need to be fulfilled.

The situation is not as clear in the low doping regime, when the K_i of the various modes flow either to zero ($i = s^-; s^+$) or to infinity ($i = c^-$). In principle it is then possible to have $K_c \rightarrow \infty$, $K_{s^+} = 0$, so by analogy with the $\cos(2\phi_s)$ term introduced by Nagaosa, we may construct interband processes of the type $\cos(2(\phi_{s^+} + \phi_{s^-}))$. The condition for these double spinon tunnellings in the interband channel to occur may be fulfilled. However one has to remember that while $K_{s^+} \rightarrow 0$ these two spin modes acquire gaps simultaneously. Thus the perturbative RG description in the LL framework cannot be valid anymore. The only firm conclusion that we may reach regards the stability of the perfectly reflecting fixed point: even if we are not in the single instanton tunnelling regime, double spinon tunnelling processes may give rise to the other instability. According to the above considerations, double holon or double spinon tunnelling events can dominate if their LL parameters are very different. This can indeed occur, since spin-charge separation is strongly enhanced by the interactions. One might thus interpret the regions of Furusaki-Nagaosa exotic tunnelling, as ones where interactions act very differently on the spin and the charge sectors (giving rise to very different K parameters). This scenario could prove even more relevant

when one turns to the quantum critical C2S2 phase. Spin-charge separation holds all the more since the eigenbases characterizing the spin and charge modes are different. Fluctuations in these two sectors are fundamentally decoupled. Higher order tunnelling processes could conceivably play a crucial role in this regime.

3.2. Boundary conditions for the phase fields

As was shown in the previous section, there exists a regime for the two-leg ladder, where the flow of the (single) impurity potential leads to a perfect reflection of the carriers in the system. This is the case of the OBC fixed point; at zero temperature, only half of the ladder is available for the motion of carriers and correlation functions around the impurity have to be modified in order to accommodate this constraint. In the framework of BCFT, this problem is solvable using a bosonic field language. Thus, for the massless LL phases, which are the main focus of this paper, correlation functions and susceptibilities can be obtained in closed analytical form (in terms of bosonic fields). For a single chain, when, because of the OBC, only the $x > 0$ half-space is available, the procedure is as follows: one writes fermionic operator in terms of the non-interacting chiral bosonic fields and then one replaces the impurity by a static, scale invariant boundary condition. This condition, corresponding to charge conservation on the exactly reflecting boundary, maps [32] a right-going field at $x > 0$ onto a left going field at the "virtual" position $x < 0$ $\phi_R(x) = \phi_L(-x)$. The theory is then written using the fields of one chirality (R or L) and, introducing the usual θ fields one gets the required correlation functions.

This scenario is quite simple for the chain, since there is only one type of reflection for fermions and hence the condition for fermionic and bosonic fields coincide. When two bands are involved the problem is more involved. Indeed, fermions can undergo intra- and/or inter-band scattering. In fermionic language, and for carriers in the α band, one may write

$$r_{\alpha} = r_{\alpha\alpha} \phi_{\alpha} + r_{\alpha\beta} \phi_{\beta} \quad (19)$$

the bosonic fields appear in the exponent of fermionic operators, so we cannot take the logarithm of both sides, as is done in the case of a chain. In order to take the band mixing term into account, we need to introduce an additional step in the procedure. From the discussion of the previous section it appears that this troublesome term (in the region of interest) close to fixed point should be much smaller than the intraband backscattering.

The aim is now to rewrite this boundary condition in bosonic field language. First we simply substitute fermionic operators:

$$\exp(i k_F x) \exp(i \phi_R) = r_{\alpha\alpha} \exp(i k_F x) \exp(i \phi_L) + r_{\alpha\beta} \exp(i k_F x) \exp(i \phi_L) \quad (20)$$

Obviously one cannot write boundary condition in the form $\phi_R(x) = \phi_L(-x)$ for the fields $\phi_{\alpha} = \phi_L(-x)$. The idea is then to write the band phase fields as a linear combination of some other fields $\phi_{\alpha} = a_{\alpha\beta} \phi_{\beta} + b_{\beta\alpha}$:

$$\exp(i(a_{\alpha\beta} \phi_{\beta} + b_{\beta\alpha})) = r_{\alpha\alpha} \exp(i(a_{\alpha\beta} \phi_{\beta} + b_{\beta\alpha})) + r_{\alpha\beta} \exp(i(b_{\beta\alpha} - a_{\alpha\beta} \phi_{\beta})) \quad (21)$$

and to find coefficients which will allow us to factorize the right hand side of (21). The final form of the right hand side will then be

$$r_a \exp(i(a_{\alpha\beta} \phi_{\beta})) r_b \exp(i(b_{\beta\alpha} \phi_{\beta})) \quad (22)$$

We have some flexibility in choosing both the $r_{a\beta}$ and $a_{\beta\alpha}$ coefficients (only their products are fixed), so using some algebra, we can find a solution to the problem

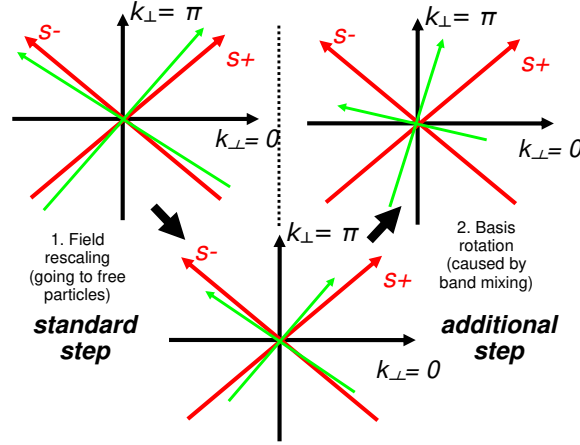


Figure 4. The two steps necessary to derive bosonic fields boundary conditions: the standard rescaling of the fields to absorb interactions and the additional basis rotation to take into account band mixing. The boundary condition is written in terms of these final fields.

namely the functional dependence of a on r_0, r_+, r_- . The factors $r_{a,b}$ can be absorbed using additional phase shifts for each field. To lowest order approximation (taking r_0 much smaller than the other r_i), we find that $b_{r_0} = r$ where $r = (r_0 + r_+) = 2$ (the average intraband backscattering).

Assuming that the fields $a_{a,b}$ are independent, we may write separate boundary condition for each of them. Taking the logarithm of Eq. (21), we find the required boundary conditions for the bosonic phase fields:

$$\phi_{La}(x) = \phi_{Ra}(x) + a \quad (23)$$

Note that these conditions are written in terms of fields defined in the new basis. Band mixing causes a rotation, and this additional step has been taken into account in Eq. (23). It was doable since we are working with the free fields. Correlation functions, in that situation, are the same for all bases, hence we choose the one that includes band-mixing.

One may wonder what would happen if one used this result for the Green functions at the LL boundary and then if we plugged them back into the equations describing the tunnelling regime. For a single mode LL, it is known [2] that, using the boundary density of states to compute the energy dependence of the tunnelling rate, yields the same result (a K^{-1} exponent in the power law) as was found in the above described instanton analysis. These exponents are taken into account in the derivation of boundary conditions by bosonic fields rescaling (the first step in Fig.4). A similar procedure can be used to confirm the second step introduced by us (bosonic modes basis rotation). The last property can be seen to hold when one evaluates tunnelling rates in the general case of arbitrary, diagonal density of states [53] (for example rotated by the presence of boundary band mixing). This result { linear dependence on band mixing } is in full agreement with our RG analysis which shows that band asymmetry suppresses interband tunnelling; so we do not need to perform further cross-checks, here.

We summarize here the main result of this subsection: the band-mixing process

was included in the bosonic boundary conditions, showing that, by and large, the single mode LL solution is stable with respect to this type of perturbation.

4. Results

Let us now present the results of our calculations. In some regimes the behavior will be similar to that observed in the case of a single chain [54, 42], but for the case of the ladder, new phenomena also occur. Furthermore, we underscore the connection between the diagonal basis found for disorder-free ladders and the nature of the regime which appears in the vicinity of a non-magnetic impurity.

Once boundary conditions are known, we may evaluate all correlation functions of fermionic operators. Thus some experimentally testable predictions of our BCFT results can be made. We will determine quantities which are relevant to STM and to NMR spectroscopies. STM will provide a local information about the charge density at some given position in the sample. From NMR experiments, one can extract some information regarding local magnetic properties around each atom. So these two techniques have the ability to give us clues about the states in the vicinity of impurities. Results given in this section mostly pertain to the intermediate and highly doped { free spinon { regimes. The low doping regime is beyond the scope of this paper. More specically, the results presented below are valid as long as OBC is a zero temperature fixed point of the RG flow (even if this behavior is masked by the presence of a gap, as is the case for the o band in the C2S1 phase). The finite temperature conformal mapping of the LL is justified as long as the zero temperature fixed point is well controlled.

4.1. Green functions

Let us start with an evaluation of local (in space) Green functions, which are important for the calculation of local density profiles. These Green functions can be readily obtained by rewriting the fermion creation operator in terms of chiral, free bosonic

$$\text{elds } \tilde{\psi}_{a=b}^L(x); \tilde{\psi}_{a=b}^R(x):$$

$$R_{0=}(x;t) = \exp(a(F(x;t;K_{0=})))\exp(-b(F(x;t;K_{0=}))) \quad (24)$$

where x is the distance from impurity and the function $F(x;t;K_{0=})$ is a standard sum of phase elds parameterized by the proper LL parameters K_i , similar to the one derived for the OBC problem in Ref. [32]. These sums can be obtained in two steps from the standard representation of R_{iL} in terms of bosonic elds ϕ_i ; ψ_i : the first step (see Fig. 4) is the standard eld rescaling to exclude interactions; in the second step one needs to go to the a - b basis in which band mixing is incorporated by the proper rotation. Then we implement the standard procedure: we use the boundary condition to introduce the $\tilde{\psi}_{a=b}^L(x); \tilde{\psi}_{a=b}^R(x)$ elds, and, at the end, we revert to canonically conjugate elds $\tilde{\psi}_{a=b}^L(x); \tilde{\psi}_{a=b}^R(x)$ where correlation functions are known. The procedure is standard [54, 55], it was even used to t numerical results for different types of 1D systems [56], and the only difference with previous calculations is the presence of a, b coefficients. Using Eq. (24), allows us to compute all correlation functions using the bosonization procedure. Spin-charge separation remains valid, so that correlations are products of charge and spin parts (for a LL, each piece is a power law with an exponent determined by K_i). They are products of a and b parts (instead of ϕ and ψ). The elds $\tilde{\psi}_{i;a,b}$ are similar to those introduced in

the case of non-interacting fermions, since all interactions were absorbed through K_i (or K_i^{-1}) rescaling, at the beginning of the procedure. Reverting to unscaled fields yields additional coefficients a^2, b^2 or ab . Note that the condition $a^2 + b^2 = 1$ has to be preserved, so that intraband correlators remain unaffected by the additional basis rotation. The new effect brought by the reflection on the impurity is the possibility of left/right correlations of fermions in different bands. This will produce some asymmetry between the two legs of the ladder. This effect causes a, b to play a role, giving an additional coefficient which changes the amplitude of the interband correlation functions by an amount $\exp(ab) \approx 1$.

For one LL mode, using CFT at finite temperature $T = \frac{1}{\beta}$, we have

$$F(x; t; V; K) = \left(\frac{1}{V} \right)^{(K+1=K)} = 4 j \sinh \left(- (t + 2x=V) \right) j^{(K+1=K)} = 8 \quad 1=4$$

$$j \sinh \left(- (t + 2x=V) \right) j^{(K+1=K)} = 8 + 1=4 \frac{\sinh \left(\frac{t}{V} \right)}{\sinh \left(\frac{2x}{V} \right)} \quad (25)$$

where x represents the distance from the boundary, and where we use units such that $\hbar = k = 1$. The propagators needed in the evaluation of correlation functions for the C2S1 phase are straightforward generalizations of those pertaining to the single chain case, and hence we get

$$\begin{aligned} h_{L0}^Y(x; t)_{R0}(x; 0) &= \exp \{ (2k_F x + \phi_0) \} \sum_{Y=0}^Y F(x; t; V_{F0}; K_0) \\ &= c; s \sum_{Y=0}^Y F(x; t; V_{F0}; K_0) \end{aligned} \quad (26)$$

$$\begin{aligned} h_L^Y(x; t)_R(x; 0) &= \exp \{ (2k_F x + \phi) \} \sum_{Y=0}^Y F(x; t; V_F; K) \\ &= c; s \sum_{Y=0}^Y F(x; t; V_F; K) \end{aligned} \quad (27)$$

These expressions allow us to reach very similar conclusions to those found previously for the single chain [55]. One easily recovers characteristic oscillating shapes, the doping dependence of the phase shift and also special features which we discussed in detail in previous sections, such as particle-hole (Fano like) asymmetries and spin-charge separation. We note that the LL parameters K in our case are usually quite close to one, and as a result the signature of the interactions is not pronounced. We also note that, at finite temperature (or frequency), one does not strictly reach the "open boundary fixed point"; this point should be especially emphasized in our case, where some of the backscattering V_b are weakly relevant.

Apart from the "standard" propagators that were introduced above, there is also an additional part connected to the band mixing

$$\begin{aligned} h_L^Y(x; t)_{R0}(x; 0) &= r_0 \exp \{ ((k_{F0} + k_F)x + \phi_0) \} \sum_{Y=0}^Y F(x; t; \frac{p}{V_F} \frac{p}{V_{F0}}; K \quad K_0) \\ &= c; s \sum_{Y=0}^Y F(x; t; \frac{p}{V_F} \frac{p}{V_{F0}}; K \quad K_0) \end{aligned} \quad (28)$$

The last component determines the difference between the chains caused by an impurity. This gives rise to a new zig-zag pattern in the vicinity of the impurity. The contribution to the LSW coming from this part has a different periodicity $((k_{F0} + k_F)^{-1})$ along the ladder than the intraband components and it alternates in

/	Cu C2S2	O centralC2S2	Cu C2S1	O centralC2S1
r_o	0.17	0.71	0.14	0.65
r	0.63	0	0.21	0
r_o	0.26	0	0.19	0

Table 1. Reflection coefficients due to defects in the C2S2 and C2S1 phases; these are calculated using the method described in Appendix C (for the two types of substitution); The values of the K_i parameters are $K_s = K_{so} = 1$, $K_{co} = 0.9$, $K_c = 0.95$ and the inverse temperature is $\beta = 1/T = 10$; the reflection coefficients increase with decreasing temperature

the y direction so it should be detectable by Fourier transform of an STM spectrum. As was pointed out in the previous section, band mixing favors -CDW instanton tunnelling and the existence of this extra part in $A(|x|)$ is in full agreement with the physical argument presented there.

These effects are illustrated on the density plots shown in Fig.5. In order to obtain a realistic plot, it is important to use the correct relative amplitudes for the various components. For that, one needs to know the values of r_{co} ; r ; r_o at some given temperature, for a given type of defect within the unit cell. We calculated these coefficients, using the method presented in the Appendix and we give their values in Table 1, for $T = 0.1$ (which, assuming $\beta = 10$, corresponds to 100K) and for various positions of the defect in the unit cell. The reflection coefficient for the on-leg oxygen atom is very similar to that of the copper atom, except for the fact that the interband reflection coefficient r_o is reduced. The amplitudes given in the table are calculated at temperatures such that the LL picture holds, and that interactions do not play a crucial role. Decreasing the energy scale will renormalize these to higher values.

The most straightforward way to determine the imaginary part of the Green function is to probe the local density of states (LDOS), using STM. Two types of measurements are available: constant voltage scan of the topography and I-V characteristics at a given atom location. The former technique is commonly used to image surface electron waves interference patterns. Using Fourier transform and filtering, one is able to extract the alternating part of LDOS which contains important information. The most interesting one in our case is the difference between profiles obtained for symmetric and asymmetric impurities. This is shown in Fig.5, where the real space, alternating, part of the LSW is shown in the contour map (as in experiments); x and y denote the on-leg and on-rung coordinates, respectively. One may clearly recognize the expected exponential decay of the amplitude, and the interference effects caused by three components with different periodicities; the pattern generated by on-leg oxygen sites is not identical to that due to on-rung oxygens, because of different decompositions into the band components. Because of the interference effect, the shape of the pattern will change with doping (the wavelengths are doping dependent). Fig.5 also shows that the effects induced by the impurity are mostly confined within a single ladder (the amplitudes on the outer oxygens are rather small). We find that, as the temperature decreases, the pattern has an increasing spatial extension and that the position of its maximum shifts away from the impurity; its shape may also change, because the relative amplitudes will renormalize. Interaction effects are not pronounced, but they control this renormalization.

Two features are worth pointing out; one is the relatively large amplitude predicted on the on-rung oxygen orbital, proving that it is important to include this

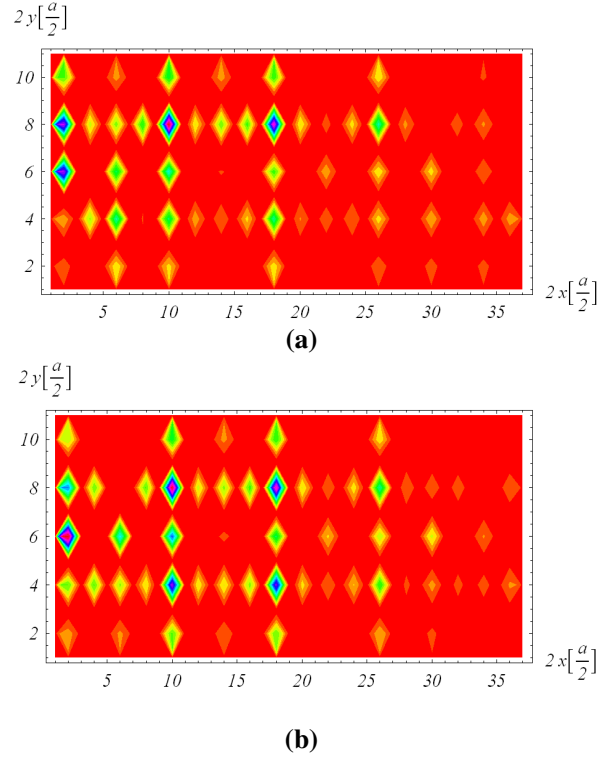


Figure 5. Alternating part of the LDOS around an impurity. The impurity sits in the cell at the left of the left boundary of each panel (hence is not shown). Interference patterns around (a) a strongly asymmetric impurity (Zn substitution of a Cu atom for example) and (b) a weakly asymmetric one (for example on-rung or apical O); $\beta = 1/T = 100$; the values of the K_i parameters are the same as in Table 1

atom in the calculation. This effect will be quite strong whenever r_o is large. The other is the presence of a zig-zag pattern, which is particularly visible for the Cu atoms which are close enough to the impurity. It shows that this kind of DW is locked on the impurity, even if band mixing is weak. This confirms the qualitative prediction that we made for the tunnelling regime. The amplitude of the zig-zag pattern will increase upon decreasing the temperature. If we take into account the fact that, by and large, asymmetric impurities reside primarily on the ladder, while symmetric ones are caused by sources external to the ladder, one is given an effective tool to recognize the nature of the impurity. Comparing bottom and top panels in Fig. 5 can thus help one identify "on-ladder" and "out-of-ladder" impurities. In our case, we find that in the bottom panel, their effect is more symmetric while the asymmetry between the legs is more pronounced in the top panel.

The latter technique in an STM experiment probes the frequency dependence of the LSW at a given site. The characteristic oscillations and particle-hole asymmetry are the effects caused by the impurity. Fig. 6 refers to the gapless situation; the minimum amplitude is obtained close to zero frequency and then it increases. For the gapped phases this feature will be shifted to frequencies of order of a gap value. This

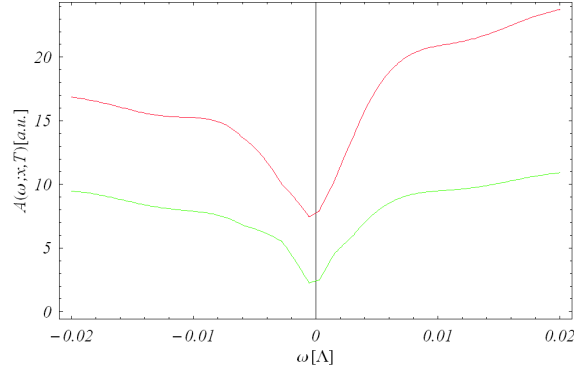


Figure 6. Frequency dependence of the LDOS measured on copper atoms (the case of non-symmetric impurity); the distance from the impurity is $x = 2$, in lattice units. Red pertains to atoms located on the same leg as that where the impurity sits, green to atoms on the the leg opposite to where the impurity sits.

effect could in principle allow one to detect the gaps if they are present in the system.

4.2. Knight shifts

As we showed in the previous section, the main effect caused by an impurity is the mixing of left and right moving carriers. This is due to the fact that, in the vicinity of the impurity, the wave vector k is not a good quantum number anymore. One can thus expect that the mixing of 0 and $2k_F$ wave functions caused by an impurity will also affect other quantities.

Let us focus on the magnetization profile given by the local, zero frequency susceptibility. Assuming that we are subjecting the sample to some external, uniform magnetic field, the 0 and $2k_F$ parts will generate alternating magnetization patterns. This effect can be detected by the changes of Knight shift for the atoms in the vicinity of the defect. Only the spin part contributes here. The uniform part does not contain band mixing terms, so we expect only intraband contributions. The expectation value that we are interested in, is $\chi_R^y = \langle \exp(i2k_F x) \exp(i\{R + L\} \frac{d}{dx}) \rangle$. This quantity is known for the single spin chain case [32], so in our case the finite temperature solution for a band (0 or π) is given by the following expression (valid in the spin-rotational invariant case, where $K_s = 1$):

$$\chi_{alt}(x) = \frac{Z_1}{1} \frac{Q \frac{1}{v} \sinh(\frac{2-x}{v})}{\int_1^{\infty} \frac{du}{u^2 + 1} \frac{1}{(u^2 - 1) \cosh(\frac{2-x}{v})}} \quad (29)$$

where x is the distance from the impurity. Eq. (29) describes a spin mode LL oscillation with a $2k_F$ wave vector around the impurity. It produces a characteristic envelope, decreasing as $1/x$ when $|x| \rightarrow 0$, and also decreasing, but exponentially, when $|x| \rightarrow 1$, with a maximum amplitude of the order of a few lattice spacings for temperatures on the order of 100K. This shape was obtained previously in the case of a spin chain [42], and we will call it wing-like, in the following.

We already pointed out [54] that the important effect caused by backscattering, in the two-band case with different wave vectors k_{F1} , is the interference – the modulation

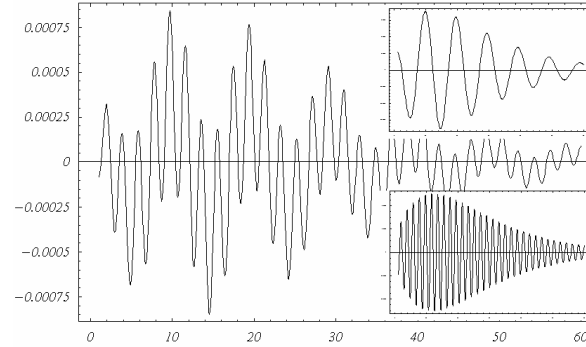


Figure 7. Interference pattern due to two intraband alternating magnetization profiles shown in the insets (magnetization, given in arbitrary units, as a function of a distance from impurity, in lattice cell units); the figure shows the amplitudes at the locations of Cu nuclei. These nuclei feel the spatially varying magnetic field which is proportional to the interference pattern. The doping is $\delta = 0.3$, and the inverse temperature is $\beta = 200$.

of alternating wings. For the static susceptibility the effect in the two chains will be the same, the reason being that the auxiliary magnetic field used as a probe is uniform and hence the same for the two chains. An example of two intraband alternating magnetizations (inset) and the resulting pattern when they are added is shown in Fig. 7 (there is no band mixing component here). As the temperature is lowered, in the case of a single chain, characteristic peaks appear on opposite sides of the main line (the reason is that for the lowest temperatures many atoms feel similar relatively strong additional fields). In the case of ladders, interference effects suppress the peaks and the distribution of local fields is more homogeneous. In the above formulae the limit of the "open boundary fixed point" was considered. In reality, there will some coefficient in front of it describing the intraband reflection. In the case of "out-of-ladder" impurities (symmetric case) the reflection in the o band is much stronger than in the π band, so that interference effects should be much less pronounced, and the broadening is quite similar to that of the single band problem.

At large distances we find an exponential decay of the alternating part, with a localization length $\xi_{loc} = v/2T$. Two conclusions can be drawn from this; one is that the broadening of the Knight shift line has a characteristic temperature dependence (the lower the temperature, the larger the number of nuclei affected by the alternating magnetization; this number increases exponentially with $1/T$ enhancing the amplitude or the broadened part). This broadening is different from the usual thermal broadening or from the temperature independent broadening due to the internal currents, in an orbital current phase (OCP). The other is that ξ_{loc} is different for the two bands (the v influence) and one has always $\xi_{loc} > \xi_{loc}^{\pi}$; this effect is strongly pronounced as one approaches the bottom of the π band. The conclusion is that with increasing doping the influence of the π band decreases.

As we have already mentioned, Eq. (29) describes how the magnetization is affected by the presence of an impurity. One of the quantities which is measured in an NMR experiment is the strength of the interaction between a nuclear spin and its electronic environment, which is usually dominated by the contact Pauli interaction between a nuclear spin and s -electrons on a given atom. To second order

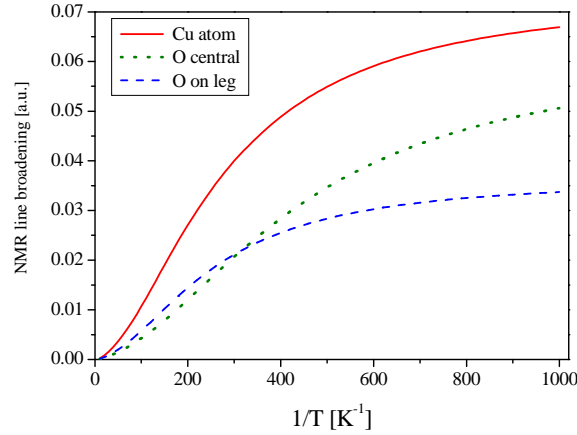


Figure 8. The integrated line broadenings on different atoms given as a function of temperature.

in perturbation, one can construct virtual hoppings of band carriers onto this core s -orbital. This process explains how uniform LL susceptibilities affect the observed NMR lines. By the same argument, we find that NMR lines (or more precisely their broadening) will be affected by the alternating magnetization induced in the band. From an experimental perspective, let us point out that, in the presence of band interferences (see Fig. 7), the shape of the broadening is difficult to predict and to distinguish from the other broadening mechanisms (in contradistinction with the single chain case).

To determine the broadening, we need to compute the hopping amplitudes between the core s - and the p,d - electronic orbitals on neighboring atoms. This was done perturbatively starting from a defect-free ladder giving us access to the broadenings for different atoms, shown in Fig. 8. Their main characteristics are as follows. The NMR line broadening of the on-rung oxygen atom (which couples only to the o band, so there is no interference) is the only one to display the characteristic shape found in the case of a single chain. The temperature dependence of the broadening is similar for all the nuclei. One can thus single out this type of broadening, by performing measurements at different temperatures. Only the linear (intermediate) part of each curve is generic. Different atoms will indeed give different slopes for the curves, since the two bands contribute differently to the wave function on a given atom. One has to remember that the large x part of $\chi(x)$ decays exponentially with a characteristic length proportional to the Fermi velocity in a given band. These band interferences will disappear with increasing doping, because the velocity in the o band becomes extremely small and only the influence of the o band remains. This effect and the different values of $\langle \chi \rangle$ (Eq. (4)) cause different slopes, but the first effect is quite easy to extract in our formalism. What remains is just the amplitude of the broadening which will change from atom to atom, providing us with information about the high momentum component of a given orbital, in the LL.

A few words about the saturation effect at very low temperatures are in order. For one single impurity, the $1/T$ temperature dependence should persist down to zero temperatures, implying that the integrated line broadening goes to infinity when

$T \neq 0$. But this situation is unphysical: one needs a finite number of impurities to detect any signal. What is more one can expect some gaps in the system (like a spin gap in the C2S1 phase, or some collective disorder effects), so there is always some low-energy cut-off. In order to account for this, we introduce an upper limit in the integral ($x_{\text{max}} = 200$ in the example above, which corresponds to the typical impurity concentration ($n = 0.005$) used in experiments). If the impurity concentration gives the low-energy cut-off scale (assuming that the Fermi velocities are known) then, from this low temperature saturation value, one can gain some insight into the density of impurities in the sample. Logarithmic corrections due to boundary operators can also be evaluated [57, 58]. They are stronger than the contributions from bulk operators ($\ln^4 T$ instead of $\ln^{0.5} T$ for $K = 1$). One might have hoped to detect these at the lowest temperatures (presumably then in the C2S2 phase. But even in that case, marginal operators are very weak in the entire critical phase, and it is not even clear that they can be detected in experiments, so we will not pursue in this direction and we omit these logarithmic corrections from hereon.

Let us briefly discuss correlation functions for two $2k_F$ operators (four fermion correlations). They are needed to obtain the NMR relaxation rate T_1^{-1} . Such correlations, including charge phase fields with $K_c \neq 1$ were evaluated in Refs. [57, 59]. In our case, as for the Green functions, 0000 , 00 and 00 terms will be present (the others are forbidden by perpendicular momentum conservation) and will produce interference patterns. This calculation (showing the behavior in the vicinity of an impurity) was done analytically for the case of two modes in a LL [59]. In our case, at high dopings, the eigenbasis is B_0 and it gives us precisely two modes (0 and 0). So we can extend the results of Ref. [59] to our problem. The result is similar to that for the static Knight shift: the lower the temperature the more atoms are affected. The problem is that the spatial fluctuation of T_1^{-1} is more difficult to access experimentally (especially when $K_i = 1$), and its temperature dependence is not so easy to analyze. There are some additional peaks with $4k_F$ periodicity but their amplitude is proportional to the interaction strength (namely $1 - K_{c+}$) so, in our case, this effect is too weak to be detected. Hence we will not consider T_1^{-1} any further, in the remainder of this paper.

5. Discussion

5.1. Experimental relevance

The above calculated alternating part of the susceptibility can be detected experimentally as an additional broadening of the NMR peaks, since the local magnetic field felt by each atom (which is proportional to the resonance frequency) will depend on its distance to the impurity.

From an experimental perspective, in order for our predictions to be testable, we need to specify the regimes where our free LL analysis applies. A short (theoretical) answer would be: as long as the impurity is strong enough a perturbation such that there exists an energy window where the results of BCFT (LL regime) can be used. In the low temperature limit, this requirement might not be fulfilled. In the C2S2 phase, higher order effects and phase stability in the vicinity of impurity might take us away from the LL state; for the C2S1 phase, the existence of a gap in the 0 band spin mode is a limitation. Last but not least, rather than a single impurity, a sample generally contains a finite concentration of defects. If these cannot be treated as independent

Influence of non-magnetic impurities on hole doped two-leg Cu-O Hubbard ladders 28

scatterers, one expects collective effects to take place. We address these issues below.

5.2. Defect in the low doping C1S0 phase

The situation is very different at low doping, where the disorder-free ladder is in the C1S0 phase. This particular limit was briefly mentioned when we discussed the RG procedure for the backscattering potential. A strong chain asymmetry emerges during the RG flow and an unpaired spin appears near the impurity. The physics, in this case is that of the Kondo problem. Here, we summarize previous attempts to describe this regime and we give some arguments which allow us to make experimentally testable predictions.

Close to half filling, and in the defect-free case, we found a phase in which all the LL modes are gapped at zero temperature, except one, corresponding to the motion of a charge soliton along the ladder. The fluctuations of the gapped modes are frozen, thus one may assume that they will adjust to a boundary (described by an unknown fixed point). The existence of this new, intermediate fixed point of the RG flow was already revealed in a previous discussion. The appearance and the on-chain nature of the boundary state was suggested. In our case, we note that, in the low temperature, unperturbed state, we have a strong, on-rung coupling. Then, we expect that an asymmetric impurity leaves one spin unpaired, such that there should exist a boundary state with spin one-half. These kind of states and their magnetic properties have already been discussed in the literature in DMRG studies [33, 37], but also analytically using reform ionization methods [39] (one works then in the space of singlet and triplet Majumara fermions). The lowest lying excitation (inside the gap) is the triplet, which corresponds to an overscreened $1=2$ spin. The magnetization profiles as well as other experimentally accessible properties of the boundary state were discussed in detail in Ref. [39]

What about the gapless c^+ mode? Spin-charge separation still holds when the impurity is present, so the above spin state will not couple to free holons at $T = 0$: the only free soliton moving along the semi-infinite ladder is the holon in the c^+ charge mode. Fermionic tunnelling events are forbidden by the fact that the lowest excitations are only of bosonic type, and, as we already pointed out, higher order tunnelling processes are not likely because all $K_i \rightarrow 1$. The problem reduces to the reflection of a soliton on a barrier, which was studied in the context of a quasi-classical sine-Gordon model [40]; since, for the other modes, the low energy physics is dominated by gaps their solution describing single soliton scattering should remain valid.

We now turn to finite temperatures. In the C1S0 phase, the LL modes are defined in the B_+ basis so that the band mixing (backscattering) effect caused by the impurity should not affect the values of the gaps. For simplicity we assume that the two spin gaps are equal. The relative magnitudes of the gaps and of the impurity potential vary with doping, but we may safely assume that upon reaching the temperature corresponding to the smaller (spin) gap (corresponding to the bosonic $s^+; s^-$ modes or singlet and triplet Majumara fermion masses), reflection is still relevant. In other words, the new fixed point, emerging because of the spin-state induced on the impurity, still dominates the physics when $T \rightarrow T_s$.

For temperatures below T_s , carriers from the bulk cannot screen the impurity spin (spin degrees of freedom are frozen). It was then suggested that the impurity can be screened by boundary states which arise from the Luther-Emery model (from a Majumara fermion picture, when both masses are positive). In that case, screening

will depend on the occupancy of this boundary state pinned at the Fermi energy. Whether or not such screening does occur depends on the relative sizes of the energies J_K and ϵ_s : if the latter is much smaller, we expect an interband Kondo regime in the SCd phase. This is a slight modification of the model with intraband J_K described in detail by Le Hur [47]. This model yields non-standard temperature dependences of the correlation functions (the screening boundary state will arise through some sort of "proximity effect"). Recall however that, for our model, all the J_K are strongly irrelevant in this regime, so that one is likely to obtain a Curie-like behavior (uncoupled impurity spin) as the temperature goes to zero.

At higher temperatures ($T > \epsilon_s$), spin degrees of freedom can fluctuate and J_K^o dominates the physics. We expect Kondo physics, as described by Eq. (18), to be relevant. This defines an interband Kondo problem with finite transmission of spinons through the impurity. Refermionization of both bulk and impurity spin degrees of freedom allows us to show that the physics in this regime is that of a resonant level model with interactions (see Appendix A for details).

At still higher temperatures $T \gg \epsilon_s$, the backscattering strength V_0 becomes weaker than the largest charge transverse gap. In such a case, which appears most likely, in view of our RG analysis, the impurity physics is totally masked by the gaps and the high temperature crossover regime (around ϵ_c) will be described by the weak backscattering potential for the soliton [60].

In the opposite case, when the impurity potential is stronger than the gaps (this can arise for very strong initial values of reflection coefficients), there exists a high temperature regime where, in principle, we should recover the results that we established in the previous sections (but this time V_0 is the dominant backscattering). Starting from the high temperature limit, we have free fermions, and, as the temperature is decreased, first we encounter an interband tunnelling regime through the barrier (still with free fermions in the bulk). As T is reduced further, the ϵ_{\pm} gaps open, singlets form on the rungs and a spin state appears on the boundary. The crossover, intermediate regime, would be described by the logarithmic corrections to the free LL [57]. The point is that this regime will appear at temperatures of order 1000K, so it is beyond the experimentally accessible range.

5.3. Defect in the intermediate doping C2S2 phase: stability in the vicinity of the impurity

The most difficult case to analyze is the C2S2 phase, since it is critical. Following the lines of our analysis for the low and high doping regimes, we would study how an impurity behaves in the C2S2 LL. However, this might turn out to be an ill defined problem. The reason is because this critical phase is extremely sensitive to perturbations. In the case of a non-magnetic impurity in a conventional metal, Friedel oscillations are generated in the vicinity of the defect. Here, a similar effect could occur, leading to some charge/spin instability. In this case the defect could induce some ordering in its vicinity and then interact with this new environment.

It is known that a finite concentration of impurities is a relevant perturbation for many 1D systems and in the next section we will explicitly show that this is the case for the Cu-O ladder as well. This type of distortion can change the phase diagram, i.e. the thermodynamic states. By contrast a single impurity, no matter how strong it is, cannot modify the bulk properties of the ladder. However we may ask whether it could lead to an instability of the phase in its neighborhood. Unfortunately, we

are in a situation where interactions and impurity backscattering are competing and momentum is not a good quantum number anymore. So, to answer the question, using a full RG analysis would require the introduction of momentum dependent vertices.

A similar question was raised in the context of a single chain problem [61] where the flow of the self-energy was obtained in a functional RG (fRG) formalism. For the flow of bulk operators, one performs RG both in momentum and frequency space, whereas for the point impurity operator, one integrates out all spatial dependence and one is left with a frequency space RG; the situation close to the boundary is somewhere in between these two limits and this is the reason why layer by layer real-space RG is necessary. There are far more couplings in the ladder problem than in the chain problem (sixteen as opposed to four), so we were not able to perform a full fRG procedure. However, under the reasonable assumption that vertex corrections do not change dramatically during the flow, we were able to connect the standard RG and fRG. Investigating possible differences enables us to make some predictions for the case of the Cu-O ladder.

Two factors affect the RG differential equations in the vicinity of a defect. One plays a role near the lower quantum critical point (QCP), on the C2S2 side of the C2S2-C1S0 border. It is the band mixing reflection which accounts for the change of the diagonal, non-interacting, basis of reflected carriers as was described in detail in section 3.2. In other words, band mixing introduces a diagonal basis for free carriers that differs from the B_0 bands. This mixing reduces the difference between Fermi velocities in the two eigen-bands, so it will change the initial P_i ; Q_i parameters in the RG equations; namely, for a given doping, the Q_i parameters will be smaller (and these coefficients decrease like r_{00}^2). This effect may be also understood if we remember that the mixing term generates an asymmetry between the chains; it can be taken into account by imposing an artificial difference between the chemical potentials, which was shown [62] to change the ratio between V_{F0} and V_F . This effect tends to shift the phase boundaries towards higher doping.

The other factor affects the upper QCP, on the C2S2 side of the C2S1-C2S2 border. This effect is slightly more subtle, and it is responsible for shifting the C2S1 boundary towards smaller dopings. In a previous section, Sec. 4.1, we showed that electron propagators change significantly in the vicinity of the impurity. So we proceed in following way: free electron Green functions enter the RG equations when, for each energy scale, we integrate out particle-particle and particle-hole instabilities $I(!)j$ (four fermion correlators). In the bulk case these two terms are proportional and their difference can be absorbed through the introduction of coefficients $\sim \frac{V_{F0}}{V_{F0}+V_F}$. When an impurity is present this simplification does not work anymore. The asymmetry between the two bands (and thus also between the Cooper and Peierls channels) will be enhanced by the following term

$$I_P - I = r_{00}^2 \int \frac{d!}{Z} I(!; V_{F0}) - \int \frac{d!}{Z} I(!; V_F) \quad (30)$$

where $I(!)$ contains an additional asymmetry caused by Fano-type, interference effects, as pointed out in Ref. [54].

The g_0 term, which is responsible for the DW gap opening in the highly doped phase, becomes even more relevant, since the mechanism that we described in the previous paragraph tends to increase the band asymmetry. This is the reason why the intraband DW phase (which dominates at large dopings) is more rigid. This can be understood as a direct consequence of the fact that the density wave, which is present

in the ground state of the C2S1 phase, can adjust its phase, and hence the charge distribution near the defect, in order to minimize the energy.

We evaluated numerically the values of both (Cooper- and Peierls- type) contributions and we found that they are of the same order. We also checked, using Table. 1, that for most of the positions of the impurity within the elementary cell, $r_{00}^2 \approx r_c^2 \approx r_0^2$. Thus, we cannot tell here which of the intra- or inter-band instability dominates, but we can make clear statements about the rigidity of the intermediate gapless phase.

Both contributions described above tend to suppress this phase and to open some gaps in the spectrum. Two additional arguments support this scenario. One is that that any marginal operator will affect correlation functions much more strongly close to a boundary. This comes from the change in dimensionality of Green's functions and it was predicted [57] to give $\log(r)^2$ instead of $\log(r)^{1=2}$ corrections to $G(r)$.

A computation of $2k_F$ instabilities, such as $\cos(kx) \cos(k_0 x)$ [57] shows that they are enhanced or suppressed close to the boundary depending on whether the bulk LL parameters K are smaller or larger than one. The analytic form of these instabilities strongly suggests that the orderings are not only favored close to the boundary but that they are also contributing to the real space RG calculations (in the same way as the fermionic Green functions $I_{p=c}$ introduced above). Based on the above considerations (taking into account the bulk values of K_i [1]), we find that, on the large doping side, a DW inside the o-band is enhanced in comparison to the other instabilities, while on the small doping side ρ_1 ; ρ_3 are enhanced and ρ_2 is suppressed. The last field describes the ρ -CDW instability. This remark is fully consistent with our discussion of the tunnelling regime; this instability corresponds to the instantons at small dopings (ρ_0 dominates) and at large dopings (ρ_0 dominates) respectively. This suggests that the results of our first order RG calculation should still hold when higher order terms are taken into account.

The following picture emerges from our stability discussion of the C2S2 critical gapless phase: it is suppressed both on the small and large dopings sides. On the low doping side it is caused by additional band mixing on the obstacle; on the high doping side it is the intraband instability which adjusts well to the presence of the impurity (and can even be enhanced in comparison with the bulk). The phase diagram that pertains to the C2S2 phase is shown in Fig.9.

The high doping side is simple { we can use a similar description to that we would give for the C2S1 phase (the dominance of the intraband LL physics with a vanishing gap in the ρ_0 mode). The spin sector remains in the total/transverse basis, but there is no gap in the ρ mode, which was a critical requirement in order to get equal couplings for the two channels and to make J_K^o more relevant than the other Kondo couplings. In addition, intraband fluctuations in the charge sector are present, which also tends to differentiate the bands. As a result, interband couplings do not dominate anymore, and a new relevant (intraband) Kondo coupling $J_K = J_K^o - J_K$ appears. The two-channel Kondo (intraband) physics is unstable with respect to band asymmetry; instead we simply expect a single channel coupling with the spin from each half-filled ladder. Because of the presence of backscattering, single-channel Kondo physics should describe this regime. The physical nature of the screening is far more traditional than in the C1S0 regime described by Eq. (18). Intraband physics can dominate even if there exists an unpaired spin-state dynamically induced on the impurity, because the BCFT framework still describes this regime, even if it is not perfectly reflecting anymore. To be more specific, if this spin-state emerges, the

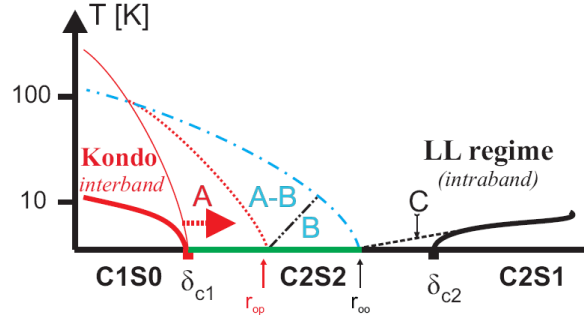


Figure 9. Influence of a non-magnetic impurity on the C2S2 region of the two-leg ladder phase diagram. Solid lines mark the temperatures below which bulk gaps develop. Dashed, dotted and dashed-dotted lines mark the cross-over temperatures of the various screening regimes observed near the impurity. A spin 1/2 is present in the impurity unit cell in the region below the blue dashed-dotted line. We distinguish the regions of interband Kondo physics (A) and single channel (o-band) Kondo physics (B) (the latter results from the channel $J_{K,o} = \text{asymmetry}$). The key observation is the transition from interband (red color) to intraband (black color) physics; the nature of the Kondo effect is different on both sides (however we predict finite, zero temperature, transmission in both cases (thick green line)). On the higher doping side there exists a region (C) of spinless o-band DW instability induced by the intraband backscattering on the impurity z ; region A arises if K_c becomes larger than one (the condition of J_o relevance); region B will appear only if neither V_o nor $V_{o'}$ are enough strong to dominate the physics.

marginally relevant instability is described by the Kondo problem, as for the critical phase of the single chain [47, 49], with some finite transmission through the impurity.

The low doping side it is also dominated by the Kondo exchange interaction, but then one expects DW fluctuations close to the impurity, because of the relevant interband interactions. As a result one would expect a similar spin screening description to that we have given for the high doping side, but emerging in the interband regime. Because of the interband r_o scattering, the low doping regime (B_+ basis) is present around the impurity, so J_K^o should be still enhanced during the RG flow. The low energy physics is then likely described by the interband Kondo terms of Eq. (18). Near the upper and lower doping boundaries of the C2S2 phase we predict finite spinon transmission through the impurity. Nevertheless, as discussed above, the physics is quite different at these two ends. Thus, there should be a phase transition somewhere in the C2S2 phase, driven by the competition between J_K^o and J_K^o . The microscopic structure of the defect, which determines the initial conditions of RG, becomes relevant, so it is difficult to predict the position and the properties of this phase transition. We leave this topic for further studies.

5.4. Influence of the spin gap in the C2S1 phase:

In the high doping, C2S1, regime the situation is quite clear; V_o (or t_o) is only marginal and the low energy physics favors the B_o basis (this is guaranteed by the existence of an intraband gap). Above the temperature scale of the gap, even in the strongly asymmetric case, the density of states on the impurity is much higher in energy than the Fermi points, which precludes the formation of boundary states. The

open boundary fixed point is thus quite robust. Some arguments suggest that this result could be extrapolated, to a certain extent, below the gap. The α and β bands are well separated then and the gap affects only the spin sector of the α band. Let us focus on this particular band (it is clear that for the β band the LL picture will hold down to zero temperature). The density wave which forms inside this band tends to get pinned on the impurity.

The opening of a gap does not significantly affect the physics around the impurity. The arguments given before, as well as results of numerical studies, rule out the possibility of a new boundary state on the impurity. From numerical studies of spin ladders, it appears that these kinds of states can appear only if the on-rung exchange energy is very different from the on-leg exchange energy ($J_{\perp} \neq J$), or in the presence of an additional strong magnetic field on the boundary. This is definitely not the case in the C2S1 phase. This statement is also in agreement with an analysis based on the boundary sine-Gordon model with $K_{\infty} = 1$ (no spinon-antiholon bound states) [40]. A picture of interfering LL modes backscattered on non-magnetic boundary emerges from this analysis.

When the scattering due to the impurity becomes strong, it simply favors a given configuration of the LL phase fields. If we assume that a gap opens, it freezes some configuration of solitons within the α mode. The opening a gap can be seen as the slowing down of this mode: the expressions that were derived before are still applicable but with renormalized velocities. Beyond this scaling limit, for the lowest temperatures one can use the solution found by Tsvetlik et al. [60]. Using spin-charge separation we find that the charge mode in the α band still gives rise to a wing-like shape of propagators, whereas the spin sector has an activated behaviour described by Bessel function of the second kind with no spatial dependence (exactly like in the bulk gapped case). As a result, the shape of the LDOS should be similar to the form predicted in the previous section, except for the fact that the maximal amplitude is shifted to a frequency ω_0 . The NMR line broadening should saturate at the lowest temperatures (there are two competing terms with exponential temperature dependences).

Despite the presence of a spin gap in both the C1S0 and the C2S1 phases, the physics is very different in the spin sector for the two phases. In particular, there does not appear to be a bound spin state around a defect in the C2S1 case, but rather a DW instability, as a result of spinon interferences. The origin of this effect comes from the presence of very different dominant boundary operators in the two states.

5.5. The many impurity case

Until now the discussion was restricted to the problem of a single impurity and to the physical effects induced in its vicinity. In this last part, we turn to the problem of a finite concentration of weak scatterers to find the effects caused by impurities acting collectively.

As for the single impurity problem, we will start with a discussion of forward scattering, which can be treated in a similar fashion to the single impurity case, using the proper shifts of the phase fields on each impurity. As for the disordered single chain, the shifts of the fields are responsible for example for the exponential decay of some density-density correlations involving α fields (it will not affect the current operator though, which depends solely on β fields, and so this effect does not correspond to weak localization). To illustrate this effect, let us take some order operator expressed

Influence of non-magnetic impurities on hole doped two-leg Cu-O Hubbard ladders 34
as a functional of bosonic phase fields, for example in the case of interband DW :

$$O_A(r) = F[c_+; s_+; c_-; s_-] \quad (31)$$

we find an additional exponential decay in the form

$$O_A(r) \sim \exp\left(-\frac{2K_{c+;s+}^2 D_f r}{V_{c+;s+}}\right) \exp\left(-\frac{2K_{c-;s-}^2 D_f r}{V_{c-;s-}}\right) \quad (32)$$

where $D_i = nV_i^2$ (as usual for gaussian, uncorrelated disorder with V_i potential on each local impurity).

The characteristic localization lengths are expected to be different for different operators and their computation is straightforward. Let us only remark, that the above formalism applies so long as a given mode is described in the LL framework (i.e. is effectively massless). In the case when an unpaired spin is induced on the impurity (Kondo regime in the low doping case) one should also take into account an additional phase shift of the s_+ field; it is the only mode which can induce impurity spin flips, which corresponds to a shift of the boundary condition.

There is one caveat. Phase shifts affect the initial conditions of the RG flow, both for the interactions and for backward scattering. As we pointed out, in the case of a single, strong impurity, backward and forward processes are independent; hence, inter- and intra-band terms may be affected in a different way, leading, for instance, to different localization lengths, from Eq. (32). This may modify the initial conditions of the backscattering contribution to the RG flow. Nevertheless, as long as we consider short range, Hubbard-type interactions, this effect can be safely neglected.

Including the backscattering part, we investigate Anderson localization { the instability of the phase diagram of the clean system to collective disorder. This problem has been discussed in the context of single orbital two-leg ladders [63] by means of a simplified RG approach. The physically relevant defect-free phases appear to be very fragile with respect to weak localization effects. An RG analysis [64] to second order in perturbation, for the half filled case, confirms this statement: in order to preserve the stability of the Mott state, one needs to choose initial values of the interaction terms several orders of magnitude larger than their disorder counterpart. Otherwise collective disorder will easily prevail during the RG flow and one observes the switchover from Mott to Anderson transition. In our case, the RG procedure follows closely that developed in Ref. [64] (see Appendix Appendix B), so we only summarize the results without going into computational details.

For the Cu-O ladder, we find that disorder terms are strongly relevant and dominate the RG flow. One new feature is revealed by our analysis; it is related to the basis rotation caused by disorder terms. One finds two generic flows in the presence of disorder:

when intraband disorder dominates we have Anderson localization for the charge modes; all interaction terms are irrelevant except g_1 and g_2 which produce a gap in the σ and π spin modes; this favors an intraband CDW order, similar to the chain problem

when interband disorder dominates, it causes Anderson localization and interaction terms are irrelevant, except g_{1a} , which favors a π CDW type order and produces a σ mixing down to the bottom of the bands

As for the discussion of interaction effects, interband instabilities are likely to dominate at lower dopings; the driving parameter is the ratio $D_{intra}=D_{inter}$ at the

beginning of the flow. One has to remember, that, until a characteristic energy scale is reached during the RG procedure, impurities renormalize as single, independent entities. In such a case the first part of the flow will determine the initial ratio $D_{\text{intra}}=D_{\text{inter}}[\zeta]$ at a scale $\zeta = n_{\text{imp}}^{-1}$.

Finally, two extra remarks about the interplay between the collective and single strong impurity limits are in order.

First, collective disorder competes with interactions (making these less relevant) so, in some indirect way, it would tend to suppress the opening of gaps at lower temperatures. For example, in the C2S1 phase, the low energy physics is dominated either by disorder or by the spin gap, and in the former case intraband solitonic states arise on each impurity (a hierarchy of breathers appears when disorder renormalizes K_{\perp} to zero). These issues were addressed in some numerical studies, but their detailed discussion is beyond the scope of the present work.

Second, as for the single impurity problem, we observe distinct small and large doping regimes. Collective and single impurity effects reinforce each other and the regions of the phase diagram where inter- and intra-band physics dominate seem to coincide for the two cases. For the high doping regime, at intermediate energy scales (where the screening clouds starts to overlap), one may expect some crossover behavior between the two power law behaviors characterized by either a single impurity or the disorder exponent. At low doping, the situation is not so clear, because of an additional flow of $K_{\perp} \rightarrow 0$ induced by disorder. Thus, the Kondo regime should be suppressed, but a detailed discussion of this effect remains an open question.

6. Conclusions

Two main results were obtained in this paper. First, correlation functions for the doped, two-leg, Cu-O Hubbard ladder in the vicinity of a single, strong, non-magnetic impurity were evaluated in the regime where the system is in a gapless LL state. In this case, these correlators can be given in closed analytical form. This means that we were able to generalize the method used to treat the equivalent problem for a single chain, to construct chiral field mappings, to handle band mixing on the impurity. Using these correlation functions, we were able to compute various magnetic response functions, which are relevant experimentally in NMR spectroscopy. We computed expressions for the local spectral response functions, which allowed us to determine the density of states versus energy on different sites. This local spectral weight is accessible in STM measurements, which makes our predictions testable. We have emphasized the different signatures of "on-ladder" and "out-of-ladder" impurities. The conclusion is that one can distinguish these two kind of impurities experimentally.

Second, we discussed and analyzed the low and high doping regimes where, at low temperature, gaps are present. We found that the impurity physics, in the low and high doping phases, is very different. The local stability of the critical C2S2 phase was also examined and we were led to conclude that the low energy physics (not protected by any gaps) is severely affected by impurities. In this respect, it is important to recall that this phase only appears because we have included oxygen atoms in the structure, and this implies that different bases describe the charge and spin fluctuations. We examined all possible scenarios for the C2S2 phase and we find that finite spin transmission takes place in some part of this doping range. This effect shows the strong relevance of oxygen atoms in the description of ladder compounds.

Finally, we considered the evolution of the phase diagram of the Cu-O ladder

when a finite concentration of weak scatterers is present. Localization effects that had been described for chains and for single orbital ladders are found here too. However, near the C1S0-C2S2 boundary, we find that new instabilities which are subdominant in the bulk may develop.

ACKNOWLEDGMENTS

This work was supported in part by the Swiss NSF under M aNEP and Division II and by an ESRT Marie Curie fellowship.

Appendix A. Interband Kondo fixed point

The Kondo problem for a LL has been extensively discussed in the literature so, in this section, we only highlight the specifics of our model. The Hamiltonian for the intraband part is known, for example from Ref. [47], in the bosonic field language

$$H_{\text{band}} = (J_z - 4\psi) S_z r_{R+} (x=0) + J_{xy} [S_+ \cos(r_{R+} (x=0)) + \text{h.c.}] \quad (\text{A } 1)$$

and this corresponds to a two-channel Kondo model.

For the interband part we find

$$H_{\text{band}} = \cos(r_{R+} (x=0)) (J_z S_z \cos(r_{R+} (x=0)) + J_{xy} [S_+ \exp(i r_{R+} (x=0)) + \text{h.c.}]) \quad (\text{A } 2)$$

The charge transverse mode dominates the RG equations. In order to evaluate the corresponding terms, we have to bear in mind that we are working with OBC, so that the scaling dimension of each chiral field is K^{-1} . Assuming that we are already at the fixed point basis B_+ (a more detailed treatment shows that this simplification is justified), we get for interband effects

$$\frac{dJ_z}{dl} = (2 - (K_c^{-1}[\ell] + K_{s+}^{-1}[\ell])) \quad (\text{A } 3)$$

where the functional $K_i[\ell]$ is known from the bulk RG flow. From previous studies of two-leg ladders [29, 30] we have that $K_c \rightarrow 1$ and $K_{s+} \rightarrow 1$ at the beginning of the flow, but $K_{s+} \rightarrow \infty$ at the end. From these observations we may infer the strong relevance of interband terms in comparison with the others.

It is also possible to reformulate our low energy spin Hamiltonian (A 2) using Kivelson's transformation: $S_+ \rightarrow U d^\dagger$ (where the Klein factor U takes care of Fermi statistics). This transformation to an interacting resonant level model enables us to extract some information regarding the thermodynamics. The result is

$$H_{\text{band}} = J_z \text{Re}[r_{R+}](x=0) (d^\dagger d - 1/2) + J_{xy} [d^\dagger r_{R+}(x=0) + \text{h.c.}] \quad (\text{A } 4)$$

Let us point out that two different fermionic operators are responsible for, respectively, interactions (first term) and hopping (second term) onto the resonant level. The interaction term does not have the usual density form.

Appendix B. System of RG equations for the disordered case

The form of the backscattering potential is the same for the single impurity and for the collective disorder cases. The only difference is the physical meaning of certain quantities; for the single, strong impurity case, V is simply the strength of the $2k_F$ component of the impurity potential; for the many weak impurity case, V is replaced by D , the density of impurities in the system, multiplied by the single impurity strength (this quantity is assumed to be non-divergent in the scaling limit). In real space it is a random variable with a Gaussian distribution, and it affects the form of the RG equations: in the former case there is no scaling in real space (in time only), whereas in the latter case one may consider that disorder spreads over the entire system. Because of this, collective disorder is able to renormalize the interactions g_i and the LLK parameters, and also to generate additional non-linear terms. All these effects were taken into account previously [64]. Our task at this point, is simply to generalize the procedure, accounting for the basis rotation, and to check whether the conclusions of Ref. [64] remain valid in the case of our doped Cu-O ladder. To that end, we introduce intraband terms D_o and D_{s+} (denoted D_{intra}) and interband terms (denoted D_{inter}). We assume that these quantities are non-zero and statistically independent.

As for the disorder-free system, when oxygen atoms are included, one needs to introduce angles of rotation of the eigenbasis with respect to the B_+ basis, through the quantities P_i ($\in [0, \pi]$) and Q_i ($\in [0, \pi]$) [30] ($i = s, c$ for the charge or spin sector). We start from the system of RG equations derived in Ref. [64] and make the following substitutions

$$K_s \rightarrow P_s^2 K_s + Q_s^2 K_{s+} \quad (\text{B.1})$$

$$K_{s+} \rightarrow P_s^2 K_{s+} + Q_s^2 K_s \quad (\text{B.2})$$

$$K_c \rightarrow P_c^2 K_c + Q_c^2 K_{c+} \quad (\text{B.3})$$

$$K_{c+} \rightarrow P_c^2 K_{c+} + Q_c^2 K_c \quad (\text{B.4})$$

For the interband term D_o (defined in the B_+ basis), and all the other "gauge" terms, this task is straightforward and the procedure does not require any further comments; as for the intraband terms, we rewrite them as $D_{o+} = \frac{1}{2}(D_o + D_{s+})$ corresponding to the operator $\cos_s \cos_{s+} \cos_c \cos_{c+}$ and $D_o = \frac{1}{2}(D_o - D_{s+})$ corresponding to $\sin_s \sin_{s+} \sin_c \sin_{c+}$ which now can be treated in much the same way as the g_o terms of the pure case [30] (these two were noted as g_1 and g_2 in that paper). The two RG differential equations describing the flow of these sum and difference of intraband backscatterings will be then slightly different from those given in Ref. [64]. We have instead

$$\begin{aligned} \frac{dD_{o+}}{dl} = D_{o+} & - \left(3 \frac{1}{2} (K_{c+} + K_c + K_{s+} + K_s) \right) \\ & + P_c Q_c (K_{c+} - K_c) P_s Q_s (K_{s+} - K_s) D_o \end{aligned} \quad (\text{B.5})$$

$$\begin{aligned} \frac{dD_o}{dl} = D_o & - \left(3 \frac{1}{2} (K_{c+} + K_c + K_{s+} + K_s) \right) \\ & + P_c Q_c (K_{c+} - K_c) P_s Q_s (K_{s+} - K_s) D_{o+} \end{aligned} \quad (\text{B.6})$$

In addition we also need to take into account the influence of disorder terms on the RG flows describing the bases rotations. Using the convention $P_s = \cos$ and

$P_c = \cos \theta$, we have

$$\frac{d \cot 2(\theta)}{d l} = \frac{((dK_{s-(c)}) - dK_{s+(c+)}) \tan 4(\theta) + dB_{s-s+(c-c+)}}{K_{s-(c)} - K_{s+(c+)}} \quad d l^{\dagger} \quad (B.7)$$

where the disorder term s cause changes both in the diagonal (standard) and in the non-diagonal parts $B_{s-s+(c-c+)}$ of Luttinger liquid compressibility matrix. The change, with respect to clean case, of the non-diagonal element (mixing i th and j th modes) is:

$$\frac{dB_{ij}}{d l} = P_i Q_i (D_o^2 (1 - K_i K_j)) - K_i K_j h[P_i] D_o - D_o + \quad (B.8)$$

The functional $h[P_i]$ is given by:

$$h[P_i] = ((P_i Q_i)^2 + 0.25(P_i^2 - Q_i^2))^{-1} \quad (B.9)$$

Appendix C . Calculation of backscattering amplitudes

In order to determine the properties of the Cu-O ladder in the vicinity of an impurity we need to determine the transmission and reflection coefficients of the barrier (ie of the unit cell containing the defect). Their values depend on the position of the defect within the unit cell { which contains two Cu and ve O atoms.

We wish to evaluate transmissions in all the channels (both intra- and inter-bands) at some finite temperature; we take the cell containing the impurity and connect it to two semi-infinite leads (ladders) described by four LL modes with arbitrary compressibility K_i . We had to assume arbitrary values, because we use $K_i[l_T]$, where the renormalization of $K_i(l)$ is stopped at the energy scale T corresponding to T . We have to work at finite temperature, because we evaluate backscattering potentials $V_i[0]$ (the initial conditions of RG flow) which then will flow towards a low energy regime ($l \rightarrow 1$).

We follow a method which is widely used in the context of mesoscopic systems. It allows one to solve 1D transmission problems and the results closely match those obtained by means of functional RG techniques [65]. We consider the Hamiltonian of the perturbed part and then introduce couplings to the leads via appropriate self energies. The retarded Green function of the i -th elementary cell (i is the distance from the defect) is obtained using Wick's equation (the bare Green functions are perturbed by hopping onto the semi-infinite leads described by the surface Green functions)

$$G_{i,i} = (E - H_i - L - R)^{-1}; \quad (C.1)$$

The Hamiltonian of the perturbed part, H_i , is explicitly introduced in this formalism, which enables us to modify it freely and to place the impurity at any chosen location in the unit cell. Self energies can be obtained from the surface Green functions $g_{i,i}^{L=R}$

$$L=R = T_{i,i-1} \sum_{i=1}^{L=R} G_{1,i-1}^{-1} T_{1,i}; \quad (C.2)$$

For the surface Green functions we take the functions derived by Eggert for the LL with OBC [54]. This allows us to include interaction effects quite easily, through changes of the K parameters; the massive mode case can also be treated using, for instance, results obtained by Tsvetlik [60]. The limitation of this method is that it uses a linear dispersion approximation (low energy limit).

The rest of the calculation is done using standard non-equilibrium Green's function formalism, under the coherent transport assumption. In the linear response

regime, the formula describing the flow of charge through the system reduces to the Landauer-Buttiker expression. The transmission function (the key quantity of this formalism corresponding to the conductivity) is:

$$T(E) = \text{Tr}(\Gamma_L(E) G(E) \Gamma_R(E) \check{G}(E)); \quad (\text{C } 3)$$

where $\Gamma_{L=R}$ is

$$\Gamma_{L=R} = \{ \Gamma_{L=R}^Y \}; \quad (\text{C } 4)$$

- [1] E. Dagotto and T. Rice, *Science* 271, 5249 (1996).
- [2] T. Giamarchi, *Quantum Physics in One Dimension* (Oxford University Press, Oxford, 2004).
- [3] C. M. Vam and Zawadowski, *Phys. Rev. B* 32, 7399 (1985).
- [4] A. Nersesyan, A. Luther, and F. Kusmartsev, *Phys. Lett. A* 176, 363 (1993).
- [5] M. Fabrizio, *Phys. Rev. B* 48, 15838 (1993).
- [6] H. J. Schulz, in *Correlated Fermions and Transport in Mesoscopic Systems*, edited by T. Martin, G. Montambaux, and J. Tran Thanh Van (Editions frontieres, Gif sur Yvette, France, 1996), p. 81.
- [7] K. Kuroki and H. Aoki, *Phys. Rev. Lett.* 72, 2947 (1994).
- [8] U. Ledermann and K. LeHur, *Phys. Rev. B* 61, 2497 (2000).
- [9] L. Balents and M. P. A. Fisher, *Phys. Rev. B* 53, 12133 (1996).
- [10] H. Lin, L. Balents, and M. P. A. Fisher, *Phys. Rev. B* 56, 6569 (1997).
- [11] Y. Piskunov, D. Jerome, P. Auban-Senzier, P. Wzietek, U. Ammerahl, G. Dhalenne, and A. Revcolevschi, *Eur. Phys. J. B* 13, 417 (2000).
- [12] Y. Piskunov, D. Jerome, P. Auban-Senzier, P. Wzietek, and A. Yakubovsky, *Phys. Rev. B* 69, 14510 (2004).
- [13] N. Fujiwara, N. Mori, Y. Uwatoko, T. Matsumoto, N. Motoyama, and S. Uchida, *Phys. Rev. Lett.* 90, 137001 (2003).
- [14] T. Imai, K. Thirber, K. Shen, A. W. Hunt, and F. Chou, *Phys. Rev. Lett.* 81, 220 (1998).
- [15] K. Kumagai, S. Tsuji, M. Kato, and Y. Koike, *Phys. Rev. Lett.* 78, 1992 (1997).
- [16] G. Kotliar and J. Liu, *Phys. Rev. B* 38, 5142(R) (1988).
- [17] S. Chakravarty, R. B. Laughlin, D. K. Morr, and C. Nayak, *Phys. Rev. B* 63, 094503 (2001).
- [18] C. M. Vam, *Phys. Rev. B* 55, 14554 (1997).
- [19] C. Vam, *Phys. Rev. B* 73, 155113 (2006).
- [20] B. Fauque, Y. Sidis, V. Hinkov, S. Pailhes, C. Lin, X. Chaud, and P. Bourges, *Phys. Rev. Lett.* 96, 197001 (2006).
- [21] Y. Li, V. Baledent, N. Barisic, Y. Cho, B. Fauque, Y. Sidis, G. Yu, X. Zhao, P. Bourges, and M. Grevin, *Nature (London)* 455, 372 (2008).
- [22] J. Xia, E. Schemm, G. Deutscher, S. Kivelson, D. Bonn, W. Hardy, R. Liang, W. Siemons, G. Koster, M. Fejer, and A. Kapitulnik, *Phys. Rev. Lett.* 100, 127002 (2008).
- [23] I. A. A. Eck and J. B. Marston, *Phys. Rev. B* 37, 3774 (1988).
- [24] P. Lederer, D. Poilblanc, and T. M. Rice, *Phys. Rev. Lett.* 63, 1519 (1989).
- [25] F. C. Zhang, *Phys. Rev. Lett.* 64, 974 (1990).
- [26] E. O. Rignac and T. Giamarchi, *Phys. Rev. B* 56, 7167 (1997).
- [27] U. Schollwöck, S. Chakravarty, J. Fjærestad, J. B. Marston, and M. Troyer, *Phys. Rev. Lett.* 90, 186401 (2003).
- [28] S. Lee, J. B. Marston, and J. Fjærestad, *Phys. Rev. B* 72, 075126 (2005).
- [29] P. Chudzinski, M. Gabay, and T. Giamarchi, *Phys. Rev. B* 76, 161101(R) (2007).
- [30] P. Chudzinski, M. Gabay, and T. Giamarchi, *Phys. Rev. B* 78, 075124 (2008).
- [31] M. Takigawa, N. Motoyama, H. Eisaki, and S. Uchida, *Phys. Rev. B* 55, 14129 (1997).
- [32] S. Eggert and I. A. A. Eck, *Phys. Rev. B* 46, 10866 (1992).
- [33] M. Laukamp, G. B. Martins, C. G.azza, A. L. Malvezzi, E. Dagotto, P. M. Hansen, A. C. Lopez, and J. Riera, *Phys. Rev. B* 57, 10755 (1998).
- [34] F. D. M. Haldane, *Phys. Rev. Lett.* 50, 1153 (1983).
- [35] N. Fujiwara, H. Yasuoka, Y. Fujishiro, M. Azuma, and M. Takano, *Phys. Rev. Lett.* 80, 604 (1998).
- [36] S. Ohsugi, Y. Tokunaga, K. Ishida, Y. Kitaoka, M. Azuma, Y. Fujishiro, and M. Takano, *Phys. Rev. B* 60, 4181 (1999).
- [37] A. Lauchli, D. Poilblanc, T. M. Rice, and S. R. White, *Phys. Rev. Lett.* 88, 257201 (2002).
- [38] T. Nakamura, *Phys. Rev. B* 59, R6589 (1999).
- [39] P. Lederer and E. O. Rignac, *Phys. Rev. B* 65, 174406 (2002).
- [40] D. Schuricht, F. H. L. Essler, A. Jafari, and E. Fradkin, *Phys. Rev. Lett.* 101, 086403 (2008).

- [41] D. Schuricht and F. H. L. Essler, *Journal of Statistical Mechanics: Theory and Experiment* P11004 (2007).
- [42] S. Eggert and I. A. A. Eck, *Phys. Rev. Lett.* 75, 934 (1995).
- [43] J. Voit, *Rep. Prog. Phys.* 58, 977 (1995).
- [44] M. Tsuchiizu and A. Furusaki, *Phys. Rev. B* 66, 245106 (2002).
- [45] C. L. Kane and M. P. A. Fisher, *Phys. Rev. Lett.* 68, 1220 (1992).
- [46] A. Furusaki and N. Nagaosa, *Phys. Rev. B* 47, 4631 (1993).
- [47] K. Le Hur, *Phys. Rev. B* 61, 1853 (2000).
- [48] M. G. Ranath and H. Johannesson, *Phys. Rev. B* 57, 987 (1998).
- [49] S. Eggert, D. P. Gustafsson, and S. Rommer, *Phys. Rev. Lett.* 86, 516 (2001).
- [50] U. Fano, *Phys. Rev.* 124, 1866 (1961).
- [51] B. R. Bulka and P. Stefanski, *Phys. Rev. Lett.* 86, 5128 (2001).
- [52] Y. Hamamoto, K. -I. Imura, and T. Kato, *Physical Review B* 77, 165402 (2008).
- [53] I. V. Krive, S. I. Kulinich, L. Y. Gorelik, R. I. Shekhter, and M. Jonson, *Phys. Rev. B* 64, 045114 (2001).
- [54] P. Kakashvili, H. Johannesson, and S. Eggert, *Physical Review B* 74, 085114 (2006).
- [55] S. Eggert, *Phys. Rev. Lett.* 84, 4413 (2000).
- [56] S. Rommer and S. Eggert, *Phys. Rev. B* 62, 4370 (2000).
- [57] V. Brunel, M. Bocquet, and T. Jolicur, *Phys. Rev. Lett.* 83, 2821 (1999).
- [58] I. A. Eck and S. Qin, *J. Phys. A* 32, 7815 (1999).
- [59] G. Wakita and Y. Suzumura, *J. Phys. Soc. Jpn.* 76, 104709 (2007).
- [60] A. M. Tsvelik, *Phys. Rev. B* 77, 073402 (2008).
- [61] S. Andergassen, T. Enss, V. Meden, W. Metzner, U. Schollwöck, and K. Schönhammer, *Phys. Rev. B* 70, 075102 (2004).
- [62] S. Wessel, M. Indergand, A. Lauchli, U. Ledermann, and M. Sigrist, *Phys. Rev. B* 67, 184517 (2003).
- [63] E. O. Rignac and T. Giamarchi, *Phys. Rev. B* 56, 7167 (1997).
- [64] S. Fujimoto and N. Kawakami, *Phys. Rev. B* 56, 9360 (1997).
- [65] A. A. Garwal and D. Sen, *Physical Review B* 73, 045332 (2006).